Numerical Simulations of Pressure effects in Passive Houses

Kunsulu Bekish

Co-promoter: prof. dr. ir. Bart Merci

Promoter: dr. Tarek Beji

International Master of Science in Fire Safety Engineering

Ghent University

2018

This thesis is submitted in partial fulfillment of the requirements for the degree of *The International Master of Science in Fire Safety Engineering (IMFSE)*. This thesis has never been submitted for any degree or examination to any other University/programme. The author(s) declare(s) that this thesis is original work except where stated. This declaration constitutes an assertion that full and accurate references and citations have been included for all material, directly included and indirectly contributing to the thesis. The author(s) gives (give) permission to make this master thesis available for consultation and to copy parts of this master thesis for personal use. In the case of any other use, the limitations of the copyright have to be respected, in particular with regard to the obligation to state expressly the source when quoting results from this master thesis. The thesis supervisor must be informed when data or results are used.

Read and approved

30.04.2018

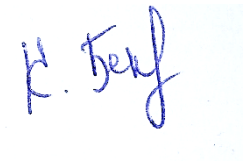

Table of Contents

List of Figures

List of Tables

Abstract

Fire-induced pressures in passive houses can hinder safe evacuation of the occupants and even lead to structural damage. Numerical study of pressure rise during fire in passive houses by using Fire Dynamics Simulator was the main focus of this thesis. The objective of the thesis was to evaluate the ability of FDS model to predict the overpressure caused by fire based on the experimental data from the testing facility built in Mons. Before the validation, preliminary leakage modelling study was performed with the focus on two leakage modelling approaches specified in FDS. The preliminary study showed the overpressure and volumetric flow through leaks are affected by the leakage modelling used in FDS as well as parameters such as area and location of the leak. For the validation study, two cases with no ventilation and with deactivated fans were considered. The analysis demonstrated that leakage area is one of the critical input parameters in FDS. Overpressure in the enclosure was better captured when the parameters such as flow exponent and reference pressure were specified. The study highlights the importance of accurate prediction of these two leakage parameters during Blower door test.

1. Introduction and Objectives

European Parliament and the Council of the European Union introduced The Buildings Energy Performance Directive which aims to decrease the energy consumption of buildings in the EU. As a result, currently there is a shift towards energy efficient buildings and passive houses. Improved insulation, air-tightness, and heat recovery ventilation are the major characteristics of passive houses. However, the concepts of energy efficiency and fire safety seem to contradict to each other as increased air-tightness can impose danger on the occupants in case of fire in well-confined enclosures. Heat released during fire leads to the pressure rise and volumetric expansion of gases. In normal buildings, pressure difference caused by thermal expansion of heated gases considered to be insignificant and normally not considered in engineering calculations due to leakage areas such as cracks and voids. However, pressure can rise considerably in tightly sealed compartments. Such increase in pressure in an air tight compartment can even lead to the structural damage that may provide additional supply of oxygen to the fire. In addition, it may hinder evacuation of occupants by preventing the opening of inward opening doors in enclosures. Therefore, more research should be done to study fire-induced pressures in airtight enclosures. The objective of this thesis is to perform numerical simulations of fires in passive houses by using Fire Dynamic Simulator and to assess its capability to predict the pressure development.

1.1 Literature review

1.1.1 Definition and requirements for passive houses

1.1.1.1 European Union

On 16 December 2002, the European Parliament and the Council of the European Union (EU) adopted The Buildings Energy Performance Directive, and it had legal power since 4 January 2003 [1]. The objective of the Directive was decrease the energy consumption of buildings in the EU. The Directive listed four major requirements for Member States:

1. Introducing the calculation methodology to estimate the energy consumption of buildings.
2. Imposing regulation that defines the minimum energy performance requirement for new buildings and large existing buildings that are planned to undergo a renovation.
3. Establishing a system to certify energy performance of new and existing buildings
4. Inspecting boilers and central air-conditioning systems on a regular basis

In May 2010, new version of the Directive was released, and it requires that the minimum standards must be met by new buildings, and efficient alternative energy systems must be present as well [2]. By 31 December 2018, new public buildings should have nearly zero-energy status, and other buildings should have a very high energy performance by 2020. As 40% to the EU's

total energy consumption corresponds to buildings, the purpose of the Directive is to contribute towards the goal of decreasing the overall energy consumption by 20% by 2020 in EU.

Enhanced insulation, air-tightness, and heat recovery ventilation are the major features of passive houses. The main purpose is limiting energy consumption for heating and cooling without compromising the comfort during all seasons. According to the Passivhaus Institute, passive houses saves up to 75% of energy in comparison with new buildings, and up to 90% can be restored compared to typical building [3]. In addition, passive house uses internal heat sources such as heat from people and appliances and heat recovery without relying much conventional heating systems. Although the location plays a significant role in the design and construction pf passive house, the basic principles behind the concept typically remain the same. Therefore, the following 5 principles should be satisfied in order to build a passive house:

1. Thermal insulation. Exterior walls, floor and roof should be well-insulated to prevent the extensive heat loss. As a result, U-value or heat transfer coefficient should not exceed 0.15 $W/m^2.K$ in colder climates, which means only heat of 0.15 watts per square meter of exterior surface and per degree of temperature difference is allowed to be lost [4].
2. Windows. The window frames should be thermally insulated and glazing should have low e-value. In addition, argon or krypton is used between glazing for better insulation [4]. For cold climates, U-value should not exceed 0.8 $W/m^2.K$ and g-value which stands for total solar transmittance should be around 50%.
3. Ventilation with heat recovery. Heat exchanger recovers up to 90% of the heat from the exhaust air and transfers it to the incoming air [5]. Thus, ventilation system provides not only fresh and clean high quality air, but also contributes to limit the energy demand.
4. Airtightness. Heat loss to the surroundings, structural damage caused by moisture infiltration, and draughts can be avoided due to airtight layer that covers the interior of passive house [5]. Especially, junctions and connections should be carefully considered.
5. Thermal bridges. The parts of structure such as edges, corners, connections and penetrations may contribute to the formation of thermal bridges which contribute to the escape of energy, as heat escapes by taking the path of least resistance [5]. Thus, thermal bridges should be avoided by thorough planning especially.

1.1.1.2 Belgium

In 2009, Belgian federal income tax legislation defined low-energy, passive and zero-energy house [6]. An income tax reduction for 10 years was introduced for dwelling owners and leaseholders

according to the legislation. Alternative energy types and corresponding calculation methods for net zero energy buildings were characterized by the Royal Decree published in 2010.

The Flanders introduced a "Energiebesluit van 19 november 2010" or "Energy decree of November 19th 2010" to comply with the Directive [7]. The Decree lists the requirements for new residential buildings, other new buildings, and existing buildings that subject to renovation.

Major requirements for nearly-zero energy buildings according to Belgian legislations include the following (Belgisch Staatsblad-Moniteur Belge, 2009) [6]

1. The overall energy demand for heating and cooling should be not more than 15 kWh/m^2.
2. The air loss should not exceed 60% of the volume of the house per hour ($n_{50} \leq 0.6$/h) which is determined by conducting a blower door test with a pressure difference of 50 Pa between indoors and outdoors.
3. Energy produced by alternative sources should be sufficient to satisfy the residual energy demand for heating and cooling.

Moreover, Belgian Passive House Platforms or Passiedhuis-Platform vzw (PHP) defines a comfort criterion [6]. For residential buildings, it is associated with occurrence of temperatures higher than 25°C being less than 5%. For non-residential buildings, the European adaptive control model EN15251 or results from physical simulations should be applied.

1.1.2 Leakage in buildings

1.1.3 Basic flow equations

Air leakage is measure of air tightness of the building shell expressed as a leakage area rather than a volume flow rate as in infiltration. The air infiltration via building envelope is governed by three factors: geometry of leakage paths (size, shape, and distribution), the flow characteristics of the leakage paths (laminar or turbulent), the pressure difference across the leakage paths [8].

Fully turbulent flow can be represented by the standard orifice flow equation:

$$\dot{V} = C_d A (2\rho \Delta P)^{0.5} \tag{1.1}$$

where $\dot{V}$ is the airflow rate (m^3/s), C_d is the discharge coefficient, A is the opening area (m^2), ΔP is the pressure difference between outdoors and indoors (Pa), and ρ is the density of air (kg/m^3).

In a sharp edge orifice flow the discharge coefficient is 0.61 as it is not affected by Reynolds number. In case of leakage through building envelope, it is suggested to use 1.0.

For the narrow openings with long flow paths, the flow is laminar or viscous [8]. The Couette flow equation for round openings applies:

$$\dot{V} = 48\,\pi r \mu L \Delta P \tag{1.2}$$

where r is the radius of opening (m), L is the flow path length, and μ is the dynamic viscosity (kg/m.s)

However, flow through leakage path is not absolutely laminar nor turbulent; thus, the following equation which is called as crack flow equation is used [8]:

$$\dot{V} = C\Delta P^{n} \tag{1.3}$$

where C is the flow coefficient which is governed by crack geometry and flow path and defined experimentally m/(s.Pa^n), and n is the flow exponent which is related to the nature of the flow through the leak. Its value varies between 0.4-1.0, and 0.65 is usually assumed for buildings [8].

1.1.4 Blower Door test

Airtightness and leakage characteristics of building envelope can be determined by performing Blower Door test which involves pressurizing or depressurizing of building zone [9]. The equipment include a fan with variable speed, airflow measuring device, and a manometer with two plastic hoses. All openings are closed during the test, and the fan speed is increased gradually to pressurize or depressurize the building, and corresponding pressure difference and airflow rates are measured. Either singe point-method or two-point method is employed for measuring and analyzing data. The former approach is associated with measuring the flow at $P_1 = 50\,Pa$ and assigning a building flow exponent to $n = 0.65$. The latter involves calculation of the building flow coefficient and flow exponent based on the flow measurements at $P_1 = 50\,Pa$ and $P_2 = 12.5\,Pa$. To characterize building airtightness, several values of reference pressures are suggested including 4 Pa, 10 Pa, 30 Pa, and 50 Pa.

Power Law equation is used to characterize the envelope leakage by defining pressure-flow relation:

$$Q_{env}(P,\rho,\mu) = C \cdot P^{n} \left(\frac{1.2041}{\rho}\right)^{1-n} \left(\frac{0.00001813}{\mu}\right)^{2n-1} \tag{1.4}$$

where C is the flow coefficient, P is pressure difference induced by blower-door (Pa), n is flow exponent, and 1.2041 kg/m^3 and 0.00001813 kg/m.s correspond to the air density and viscosity at 20℃,respectively.

Flow exponent is calculated by using Eq. (1.5):

$$n = \frac{ln\left(\frac{Q_{env1}}{Q_{env2}}\right)}{ln\left(\frac{P_1}{P_2}\right)} \tag{1.5}$$

where Q_{env1} is average air leakage rate at the primary pressure station, Q_{env2} is average air leakage at the secondary station, P_1 is average pressure at primary station, and P_2 is average pressure at secondary station.

Depending on either depressurizing or pressurizing the enclosure, flow coefficient is estimated by using Eqs. (1.6) and (1.7), respectively:

$$C = \frac{Q_{env1}}{(P_1)^n}\left(\frac{\rho_{out}}{\rho_\infty}\right)^{1-n}\left(\frac{\mu_{out}}{0.00001813}\right)^{2n-1} \tag{1.6}$$

$$C = \frac{Q_{env1}}{(P_1)^n}\left(\frac{\rho_{in}}{\rho_\infty}\right)^{1-n}\left(\frac{\mu_{in}}{0.00001813}\right)^{2n-1} \tag{1.7}$$

where $\mu_{out}$and μ_{in} is dynamic viscosity of air outdoors and indoors.

Therefore, by using estimated flow exponent and flow coefficient, effective leakage area is defined, L (m^2):

$$L = C \cdot P_{ref}^{(n-0.5)}\left(\frac{\rho_e}{2}\right)^{0.5} \tag{1.8}$$

where ρ_e is standard air density, 1.2041 kg/m^3, and P_{ref} is selected reference pressure. The ASHRAE Handbook of Fundamentals uses 4 Pa; thus, the values are extrapolated for 4 Pa which might lead to inaccurate predictions because of using the relation between pressure and the air leakage rate. According to [9] the uncertainty for extrapolated flow at 4 Pa is 13%, while 10% of uncertainty for flow coefficient and 0.05 for flow exponent would be expected.

1.2 Experimental studies

1.2.1 OECD PRISME

Smoke and heat propagation in multi-compartment fires and their effect on electrical cables were studied in the framework of OECD, Organization for Economic Co-Operation and Development, PRISME fire research project [10]. As a result, 35 large scale tests as part of 5 experimental campaigns such as PRISME SOURCE, PRISME DORR, PRISME LEAK and PRISME INTEGRAL were conducted with participation of several international organizations in 2006-2011.

Pressure profiles in PRISME fire tests consisted of ignition overpressure peak, oscillations and/or other high pressure values at the combustion, and extinction low pressure peak. To illustrate, for PRISME SOURCE test configurations, the highest pressure difference of 2963 Pa and the lowest pressure difference of -2613 Pa were measured [11]. According to theoretical analysis, heat release rate, heat lost to the surroundings and the net energy balance through the ventilation branches are constituents of energy balance which cause pressure variation in the compartment. Parameters including thermal properties of the enclosure, coefficients of airflow resistance of the ventilation system and development of fire with time were found to govern the pressure.

The tests showed that air flow in ventilation system changes with pressure values. High pressure creates an increase of the exhaust flow rate and reduces the inlet flow rate, whereas low pressure values cause an opposite effect. In addition, flow can be inversed either when pressure in compartment is high or low compared to the inlet and outlet pressures during ignition and extinction, respectively. As a result, oxygen supply via inlet duct can be hindered at ignition which leads to the under-ventilated fire conditions, while re-ignition might take place at extinction due to fresh air coming from exhaust in case of presence of adequate amount of fuel for combustion. Therefore, PRISME fire tests indicated that in confined and ventilated compartment pressure changes play a considerable role in fire development.

1.2.2 FLIP test

Pretrel et al. [11] studied how pressure varies in a well-confined and mechanically ventilated enclosure based on large-scale hydrocarbon pool fire experiments conducted by ‘‘Institut de Radioprotection et de Suˆ rete´ Nucle´aire’’ (IRSN). Experiments were performed as part of FLIP and PRISME SOURCE research programs in 400 m^3 and 120 m^3 air tight compartments. Both enclosures had mechanical ventilation with inlet and outlet branches, but unlike in PRISME SOURCE experiment no fan was installed in the inlet branch of the FLIP test. According to the test results, typical behaviour of overpressure and underpressure can be observed during ignition and extinction phases of fire, respectively. For FLIP test, the highest overpressure was 3500 Pa, and the lowest underpressure was -1026 Pa. The overpressure peak was explained by the unbalance of HRR, while thermal losses, increase in ventilation flows, and stabilisation of the HRR of the fire were listed as the causes of pressure decay.

1.2.3 FOA series

FOA series comprised of the following two sets of tests: pressure increase induced by fire growth in a closed room (1996) and smoke spread via ventilation ducts (1998). Three tests were carried out in the frame of the first series with t^2 fires of varying growth rates in a room with an

opening, but without ventilation network. The second set consisted of three series of tests to study the smoke spread via ventilation ducts with different configuration: with no ventilation, with only exhaust ventilation, and with both supply and exhaust ventilation. In all tests, N-Heptane in 0.73m x 1m fuel pan was used as a fire source. HRRPUA was calculated as 1600 kW/m^2. Based on the results of 1 test configuration (1996), positive relation was observed between the fire growth rate and peak overpressure, and for fast growing fires peak pressure values higher than 100 Pa were measured. The highest measured pressure peak was 1200 Pa in FOA experiments.

1.2.4 Aalto experiments

Aalto experiments consisted of thirteen full scale tests carried out in apartment building constructed in 1970s. The purpose of the experiment was to examine how different ventilation conditions influence the pressure development in the apartment with fire. Depending on the fuel type used, namely liquid or solid, tests were carried out in two phases. Average peak temperatures of gases were 150°C, while up to 300°C peak temperatures were measured during the tests. The experiments have shown that pressure can rise and decline substantially depending on the ventilation configuration in relatively closed compartments. The over-pressure values increased up to 600 Pa when normal valves were installed to open ducts, whereas 900 Pa peak pressures were measured for closed ducts. The tests results showed that the effect of the fan is insignificant for pressure values. Regarding the fuel type, solid fuel fires (PUF mattress) caused higher over-pressure values with the maximum value of 1650 Pa in comparison to the heptane pool fires. Such high overpressure was obtained when the fire was in the closet, and it caused the failure of the wall separating the balcony and the living room. In addition, during the test with PUF mattress, the firefighter who ignited the fuel experienced a problem with opening the door and escaping the apartment. This showed that high pressures during a fire can hinder evacuation of occupants.

1.3 Numerical modelling studies

1.3.1 Fire Dynamics Simulator

Wahlqvist and van Hees [12] used FDS to simulate the OECD experimental results. It was concluded that overall the fire-induced pressure rise was accurately predicted by FDS. Nevertheless, the discrepancy between the experimental and computational results was indicated in some cases due to poor characterization of loss coefficients values. Therefore, the sensitivity of the ventilation system was noted. In addition, in several occasions the FDS model inverted the inlet flow at lower pressures compared to the experiment. Authors deduce that this might have been caused by the incorrect test measurement or by the change in some parameters of the system. Furthermore, FDS model captured the initial peak pressures in some of the tests which were not

observed in the experiment. Authors suggest that this discrepancy is caused by the variance between the measured mass loss rate and actual HRR during the test.

Experimental data obtained during FOA and Aalto fire tests were validated by using FDS by Kallada Janardhan [13]. FDS simulations of FOA experiments revealed the general trend of over-pressure values being better captured by the model compared to the under-pressure values [13]. It should be noted that the peak temperatures were over-predicted when the experimental data from the first set of FOA experiments (1996) were simulated. The leakage was modelled by using HVAC duct in the validation of FOA test results, and the pressure values were not affected significantly when the localized leakage model was used to check the sensitivity.

When Aalto experiments were simulated using FDS, the pressure in the compartment varied depending on the adopted leakage modelling method including the HVAC, Localized and Pressure Zone (Bulk) leakage methods. Bulk leakage model overpredicted the pressures in enclosure, while pressure values were lower when the Localised leakage and HVAC leakage methods had been used. Regarding the ventilation flow, outward flows were better simulated by FDS. Nevertheless, the reverse flow after the burnout was not predicted by the model.

For validation of FOA test series and Aalto experiments, FDS model gave in average 11% higher temperature values compared to measured temperatures during the experiments. Authors claim that it is acceptable by taking into account the uncertainties regarding the HRR. Underprediction of exhaust gas temperatures was also noticed due to inability of FDS model to consider heat transfer to the duct. Moreover, it was concluded that FDS poorly predicted CO yield due to simple chemistry model.

Hostikka et al. [14] examined the impact of air tightness on development of fire pressures by performing numerical simulations in hypothetical apartment buildings with various air-tightness. By introducing changes to fire growth rate, envelope air-tightness, and damper configuration 34 simulations were performed.

Table 1.1. Parameters for numerical simulations [14]

Parameters			
Fire growth rate	Medium: Max HRR=4 MW, tg=300s	Fast: Max HRR=4 MW, tg=150 s	Ultra-fast: Max HRR=1 MW (experimental), tg=70 s

Air tightness	‘Traditional’: average of the required and reference values	‘Modern’: corresponding to the concrete multiple storey buidling	‘Near-zero’: current level that can be reached
Damper configuration	Off: inlet and outlet kept open during fire	Inlet: 10 s after ignition the inlet duct was closed	Both: both inlet and outlet were closed 10s after ignition

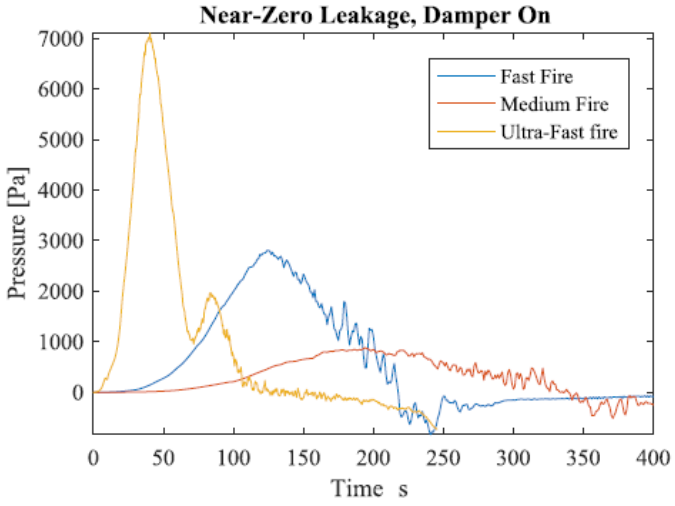

Figure 1.3.1. Pressure development (near zero leakage and damper on) [14]

The highest pressure values were obtained in case of air-tight (‘near-zero’) compartment and when both inlet and outlet were closed. The correlation between the peak overpressure and fire growth rate was determined: as Figure 1.3.1 shows, ultra-fast fires led to 7000 Pa, while 3000 Pa and 1000 Pa were developed for fast and medium fires [14]. 100 Pa overpressure can prevent occupants to open a door in a compartment with fire, and lightweight structures tend to fail at 1450-1600 Pa overpressure. Therefore, the study showed that the problem with door opening can take place in ‘modern’ and ‘near-zero’ apartments, while damage to the structural integrity of the building is likely to occur in air-tight buildings with closed ducts. 100 Pa pressure values were achieved in 1-3 minutes after ignition for fast developing fires and in 2-3 minutes for medium fires. In addition, overpressure in apartment lasted up to 4 minutes [15]. Hostikka et al. also revealed that parameters became more sensitive for a scenario with high values of overpressure. To illustrate, the role of damper configuration is more important for air tight buildings in comparison to normal buildings. The results have also demonstrated that pressure rise is not governed by fan configuration (on or off) and position of the fan unit damper. To prevent the smoke spread to neighbouring apartments, closing the inlet duct and leaving the exhaust open was found as the most appropriate ventilation configuration.

1.3.2 Pressure Rise Simulator

Li [16] developed a model named Pressure Rise Simulator (PRS) to simulate the pressure rise due to fire in a well-sealed single room with either natural or mechanical ventilation. The model was used to validate the FOA (1996) test results conducted by the Defence Research Establishment to study the "pressure rise due to fire growth in a closed room". In addition, PRS results were compared with FDS simulation results. It was shown that PRS simulation results were in agreement with the test results both in case of over-pressure and under-pressure in contrast to FDS which cannot capture the pressure decrease at extinction. FDS simulations were performed by using different methods including using extinction model (default), introducing ignition models, deactivating both ignition and extinction model. Nevertheless, ignition model caused overprediction of pressure rise, while defining extinction time is complicated; thus, extinction model was kept by the default for further comparisons. Moreover, oxygen concentration and gas velocity in duct were recreated with accuracy by PRS model. The results revealed the correlation between the size of the compartment and the fire-induced pressure profiles in a compartment. To illustrate, higher over-pressure and under-pressure values were observed when the room is large. The results have also noted the impact of the fire growth rate on the pressure rise, whereas the pressure drop is not affected considerably. Furthermore, the study also reported that fire size has a limited impact on the variation of the pressure values. Although the positive correlation was observed between fire size and the pressure rise for small fires, at certain fire size this correlation is no longer valid. In rooms where natural ventilation is present, the importance of the opening areas was remarked. In case of the room with mechanical ventilation, both inlet and outlet ducts mostly acted as exhaust due to high values of pressure rise. However, when the pressure rise in the room was lower than the supply pressures, due to the inflow of the air the pressure in enclosure increased. As a consequence, depending on presence of natural or mechanical ventilation, it is recommended either to increase the opening area or terminate the supply and decrease the exhaust pressure, respectively.

1.3.3 CFAST

The study was conducted by University of Mons and funded by the Ministry of Interior of Belgium [17]. The goal was to identify how parameters such air tightness, thermal insulation and mechanical ventilation influence fire spread and smoke propagation. Two-zone model, CFAST, was used to simulate and compare models of a traditional house and an existing passive house in Belgium. Different materials were chosen for interior lining, and two additional compartments were added for ventilation purposes for the air-tight compartment model. For both models, a standard sofa was selected as a fire source. The results have shown that although at the ignition fire growth was similar in both cases, fire in a passive house model stopped to develop after 6

minutes from ignition because of insufficient amount of oxygen. The results have shown lower fume temperatures, but an increased amount of incomplete combustion products in case of the passive house. Figure 1.3.2 shows the comparison between pressure variation in traditional and passive houses. It can be seen that pressure in traditional house remains steady at near 50 Pa throughout the simulation time except small peaks after 8 and 10 minutes from ignition. In case of passive house, pressure rises and peaks at about 500 Pa in the initial phase of the fire, but drops drastically resulting in peak under-pressure of 200 Pa. Thus, the results of this simulation also showed that the pressure rise greater than 100 Pa which is essential for a safe escape of occupants is exceeded in passive house.

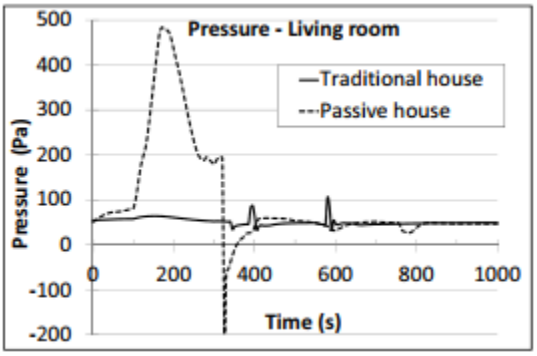

Figure 1.3.2. Pressure inside a living room [17]

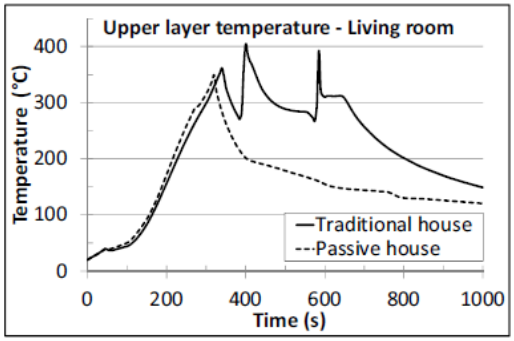

Figure 1.3.3. Upper layer temperature in a living room [17]

Figure 1.3.3 shows the temperature profile in upper layer, and it can be observed that both in traditional and passive houses have similar development of temperature reaching about 350^{o}C at 300 s. However, in passive house, it is followed by the decline, thereby temperatures in the upper layer of living room in passive house were found to be lower compared to the traditional house. It should be noted though that ignorance of a pyrolysis model is the limitation associated by using CFAST model as the radiative effect of flames on the rate of pyrolysis was not considered.

2. Methodology

2.1 Mons experiments

2.1.1 Scenarios

6 preliminary tests with varying fuels and ventilation configuration were conducted in 2016 by Berthelot [18] based on the thesis of Vanhaverbeke [7]. Nevertheless, the tests results were not coherent: HRR values were not repeatable due to difference in the arrangement of wooden pallets and their humidity. As a result, new set of experiments were carried out to better capture the fire development in the well-insulated enclosure. It should be mentioned that based on the blower door test measurements, the building did not comply with the requirement of 0.6 vol/h renewal rate at a pressure difference of 50 Pa: the value was around 1 vol/h.

Four tests were carried out with different ventilation conditions. In three tests, 38 cm long pine slats with 27x18 mm^2 cross-section were used as a fuel. For Test 4, larger fire was used as shown in Table 2.1. It should be noted that during the experiments 100 ml of heptane in a 95 mm diameter cup was placed under the pine slats to produce an appropriate heat flux for ignition. As Tests 1 and 2 were under analysis in the master thesis of Orozco Cruz, this work will focus on Tests 3 and Test 4.

Table 2.1. Test scenarios

	Fire source	Ventilation
Test 1	15 layers of pine slats 380x27x18 mm^3	No mechanical ventilation and closed pipes
Test 2	15 layers of pine slats 380x27x18 mm^3	Mechanical ventilation is on
Test 3	15 layers of pine slats 380x27x18 mm^3	Fans off and open pipes
Test 4	15 layers of pine slats 594x30x17 mm^3	No mechanical ventilation and larger fire source

2.1.2 Configuration

The experiments were carried out in a building with the following inner dimensions: length of 12.03 m, width of 2.35 m, and height of 2.39 m [7]. The building sits on a concrete slab foundation

and walls are made of 20 cm concrete blocks, and the interior of concrete blocks was covered with plaster to make a building air-tight. In addition, steel studs with the width of 4.5 cm were placed and 5 cm mineral wool was used to fill the cavities between the metal studs. Two 13 mm thick plasterboards were installed after steel studs. The outer plasterboard was replaced after each test since thermal properties of plasterboard alter when it is exposed to the temperatures higher than 80^0C [7]. The ceiling was made of cast in situ concrete slab, and only 3 m of it was insulated with mineral wool and plaster board for practical reasons: as they have to be replaced after each test which requires more effort at the ceiling compared to the walls. The major reason for insulating the ceiling was to decrease the significant heat losses.

The building was divided into two rooms, and one room has inlet duct, while the exhaust duct was placed in the other [7]. The room where fire will be set is larger compared to the other room, 18.8 m^2 and 9.4 m^2, respectively. It was assumed that the larger room is a living room, while the smaller room is a bathroom. The ventilation opening was made between two rooms under the door. Supply and extraction fans that are usually installed in the residential buildings were used in this experiment. To preclude a significant impact from wind, the fans will be installed in a partially sealed environment.

The decree published in Flanders named *"Energiebesluit van 19 november 2010"* or "Energy decree of November 19th 2010") sets the requirement on minimal and maximum nominal flows based on the occupation in passive houses [7]. According to that minimal flow rate should be 75 m^3/h in living rooms and 50 m^3/h in small rooms such as kitchens, washing rooms and drying rooms. Therefore, it was decided that installed fans must provide at least 80 m^3/h or 22 l/s design flow. The ventilation ducts are made of 100 mm dimeter galvanized steel pipes.

2.1.3 Measurements

Pressure in a test facility was measured by using 2 manometers: one was placed between the fire room and adjacent room, whereas the other was installed between the room in fire and outdoors [18]. Moreover, to measure the pressure difference at the adjustable ports, 2 other sensors were installed in the ventilation ducts.

To measure temperatures, 2 thermocouple trees with 11 units and 7 independent thermocouples were distributed throughout the facility [7]. As a result, 29 thermocouples were installed in total. Temperatures over the height in both rooms were captured by the thermocouple trees. Thermocouples were also placed every 60 cm on the plasterboard wall, and one thermocouple was installed at the back of the plasterboard as well. 2 more thermocouples were located close to orifice plates in supply and extraction ducts, and the last thermocouple was put right above the fuel. K

type thermocouples were used in the experiments due to low cost, high reliability, and wide temperature range (-270^{0}C and +1370^{0}C).

To ensure the specified flow rate of air in the ducts, an adjustable orifice plate DIRU 100 which is manufactured by Lindab was installed [7]. Parameters related to the orifice plate, setting factor and resulting k factor, should be selected iteratively, so that the pressure drop corresponding to the required flow is achieved.

Mass flow rate was measured by using strain gauges, as product of mass flow rate and heat of combustion of the fuel gives the HRR [18]. Lifting device comprising of four weighing sensors able to measure up to 220 kg was used. As the sensors were supposed to be exposed to high temperatures, the sensor protection box similar to the one in the experiment conducted by Svensson in 2002 was adopted. As a result, PROMATECT H fire-resistant plated were supported by the metal frame. In order to convert the voltage signal provided by the weighing sensors, an electronic converter was applied.

Gas analyzer was located at the thermocouple shaft in fire to measure the concentrations of oxygen, carbon monoxide, and carbon dioxide [18]. The measurement ranges for O_2, CO, and CO_2 were 0-21%, 0-15%, and 0-1%, respectively. However, after the tests were conducted, it was found out no measurements were made by the gas analyzer.

The testing facility was also equipped with detection system, namely with optical smoke detectors, corresponding to the requirements set by the European Standards [7].

2.2 Fire Dynamics Simulator

According to the User's guide of Fire Dynamics Simulator, it is "a computational fluid dynamics (CFD) model of fire-driven fluid flow [19]." By using FDS, the form of Navier-Stokes equations for low-speed, thermally-driven flow is solved numerically. Finite differences represent the partial derivatives of the conservation equations of mass, momentum and energy, and three-dimensional, rectilinear grid is used to update the solution [20]. Thermal radiation and the flow solver are estimated on the same grid by employing a finite volume technique. Objects that are too small to be resolved on the numerical grid such as smoke particles are liquid droplets are represented by Lagrangian particles. FDS is used with Smokeview which is a visualisation tool that produces images and animations of the results obtained by the former. Table 2.2 shows the short description of the major features of FDS [19].

Table 2.2. Brief summary of basic FDS features

Models	Description
Hydrodynamic model	Explicit predictor-corrector scheme, 2nd order accurate in time and space Turbulence is treated by Large Eddy Simulation (default)
Combustion model	Single step, mixing-controlled chemical reaction
Radiation transport	Radiation transport equation solved for a gray gas

2.2.1 Pressure modelling

Due to the scope of the thesis, the following paragraphs will describe how pressure, ventilation, and leakage are modelled in FDS. Pressure in FDS is comprised of two components, background pressure, $\bar{p}(z,t)$,which is a hydrostatic pressure and perturbation pressure, $\tilde{p}(x,y,z,t)$,which is induced by the flow and resolved spatially [21]. Dividing the absolute pressure into components allow each compartment to have separate background pressures, and differences in background pressures can be used to define air flows between compartments. The latter eliminates the necessity to deal with complicated flow equations in the ventilation duct. This approximation is called low Mach number approximation. The background pressure is used in the ideal gas law to filter out high speed sound waves due to low Mach number approximation [21]:

$$\bar{p} = \rho RT \sum_{\alpha} \frac{Z_\alpha}{W_\alpha} \equiv \frac{\rho RT}{W} \tag{2.1}$$

where Z_α is the mass fraction of lumped species α

Low Mach number approximation allows to use thermodynamic background pressure to define internal energy and enthalpy. As a result, energy conservation equation is expressed in terms of the sensible enthalpy, h_s [21]:

$$\frac{\partial}{\partial t}(\rho h_s) + \nabla \cdot (\rho h_s \boldsymbol{u}) = \frac{D\bar{p}}{Dt} + \dot{q}''' - \dot{q}_b''' - \nabla \cdot \dot{\boldsymbol{q}}'' \tag{2.2}$$

where $\dot{q}'''$ is the HRRPUV due to chemical reaction, $\dot{q}_b'''$ is the energy received by subgrid-scale droplets and particles, $\dot{\boldsymbol{q}}''$ defines heat fluxes by conduction, diffusion, and radiation. The energy equation is not solved in an explicit manner: the velocity divergence (the rate of volumetric expansion) is $\nabla \cdot \boldsymbol{u}$ used in hydrodynamics solver.

Background pressure is governed by vertical spatial coordinate and time [21]. Nevertheless, it does not vary significantly with height and time in most of compartment fires, except in the presence of

HVAC system, in case of air-tight (closed) compartments and in case of substantial height of domain. Eq. (2.3) is used to estimate the variations in the background pressure with time:

$$\frac{\partial \bar{p}_m}{\partial t} = \int_{\Omega_m} D\ dV - \int_{\partial\Omega_m} \boldsymbol{u} \cdot d\boldsymbol{S} \Big/ \int_{\Omega_m} P\ dV \tag{2.3}$$

where subscript *m* refers to the number of the pressure zone and Ω_m is the zone volume.

The perturbation pressure governs the fluid motion [21]. It is used to solve the momentum equation by correcting the velocity fields. It appears in an elliptic partial differential equation which is also named as a Poisson equation. This equation is solved by using a direct FTT-based solver.

2.2.2 Ventilation modelling

Heating, Ventilation and Air Conditioning can be modelled in FDS by using simple velocity boundary conditions or by using HVAC solver [19]. The former can be used to specify air flow rates into and out of compartment, while the latter should be used if the entire HVAC system is to be modelled. When the heat and combustion transfer of products through duct network and pressurization of a compartment due to fire and ventilation flows in ducts are under consideration, HVAC solver should be employed [19].

HVAC solver is based on the MELCOR thermal hydraulic solver which implicitly solves momentum conservation equation while mass and energy conservation equations are solved in explicit manner [21]. Network of nodes and ducts form an HVAC system in FDS. Currently, mass storage within an HVAC network is not considered by the model. The nodal conservation equation for mass, energy, and momentum are listed below:

$$\sum_j \rho_j u_j A_j = 0 \tag{2.4}$$

$$\sum_j \rho_j u_j A_j h_j = 0 \tag{2.5}$$

$$\rho_j L_j \frac{du_j}{dt} = (p_i - p_k) + (\rho g \Delta z)_j + \Delta p_j - \frac{1}{2} K_j \rho_j |u_j| u_j \tag{2.6}$$

where u is the flow velocity in the duct, A is the duct area, and h js the enthalpy of the fluid in the duct. Subscripts i and k correspond to the nodes, while j corresponds to the duct. Fan or blower, which can be considered as a source of momentum, is indicated by Δp, the length of the duct segment is defined by L, and K is the loss due to friction in the duct.

Based on the mass and energy conservation equations, inflow into a node equals to outflow out of a node as node have no volume . Pressure gradient across the nodes, the buoyancy head, externally increased pressure (due to a fan or blower), and effects of wall friction and duct fittings expressed as pressure losses are terms in the right-hand side of the momentum equation.

2.2.3 Leakage modelling

HVAC solver can be also used to model leakage, as leakage cannot be directly defined on a numerical mesh due to the small size [19]. Therefore, HVAC model is usually used to introduce leakage: HVAC vent with a small duct corresponds to the leaking surface. As a result, leakage area is well depicted, and leakage occurs over a large area in the computational domain. This way of leakage modelling can be achieved by two methods.

2.2.3.1 Pressure zone (bulk) leakage

The first is associated with pressure zones which is a user-defined volume outlined by solid obstructions within the computational domain [19]. In this case, surfaces in the pressure zone through which leakage occur can be accounted as an HVAC vent and leakage area represent a duct. This method precludes significant pressure variations during the fire development, and it is known either as Pressure Zone Leakage or Bulk Leakage. By adopting this method, it is assumed that the leaked air will have identical temperature as the wall surface due to insignificant amount of leaked air and extensive heat exchange.

According to the FDS User's Guide, the volume flow rate through a leakage is expressed as:

$$\dot{V}_{leak} = A_L sign\,(\Delta p)\sqrt{2\frac{|\Delta p|}{\rho_\infty}} \tag{2.7}$$

where A_L is a leak area, Δp is pressure difference (Pa), and ρ_∞ is the ambient density (kg/m^3). Volume flow rate can be post-processed by using 'DUCT VOLUME FLOW' output device. Therefore, measured and calculated volume flow rate through leakage will be compared in this section.

To take into account increase in leakage area as pressure rises, `LEAK_PRESSURE_EXPONENT` (n) and `LEAK_REFERENCE_PRESSURE` (Δp_{ref}) should be defined in the input file. These two parameters are used to define the leakage area by using the following equation:

$$A_L = A_{L,ref}\left(\frac{\Delta p}{\Delta p_{ref}}\right)^{n-0.5} \tag{2.8}$$

where $A_{L,ref}$ is leak area defined by `LEAK_AREA`, A_L is updated leak area. $n = 0.5$ and $\Delta p_{ref} = 4\ Pa$ are the default values. It can be seen that variation of leak area with pressure is not considered when the default `LEAK_PRESSURE_EXPONENT` is used.

2.2.3.2 Localized leakage

The second method is appropriate when the leakage locations are specified [19]. The magnitude of leakage can change, as this method exploits local pressure. Unlike Bulk Leakage, Localized leakage can be used to take into account stack effect. Moreover, by adopting this method, the temperature of the gas leaking out can be determined. For Localized leakage, leakage flow is governed by local pressure at the vent which combines hydrostatic and perturbation components, whereas background pressure is the driving force for the flow in Bulk leakage method.

2.3 Leakage modelling study

Before starting the validation of experiments, it was decided to study the leakage modelling approaches in hypothetical closed room with adiabatic surfaces. The aim of the study is to focus on two leakage modelling approaches, pressure zone leakage and localized leakage, and to observe how pressure and leakage flows are affected by the location of leakage path and varying parameters like pressure exponent values.

2.3.1 FDS version

Leakage modelling study was performed by using FDS 6.5.3 version.

2.3.2 Geometry

The geometry of ISO room with the 3.6 m x 2.4 m x 2.4 m dimensions was adopted for the leakage modelling study. All surfaces were assigned to be adiabatic.

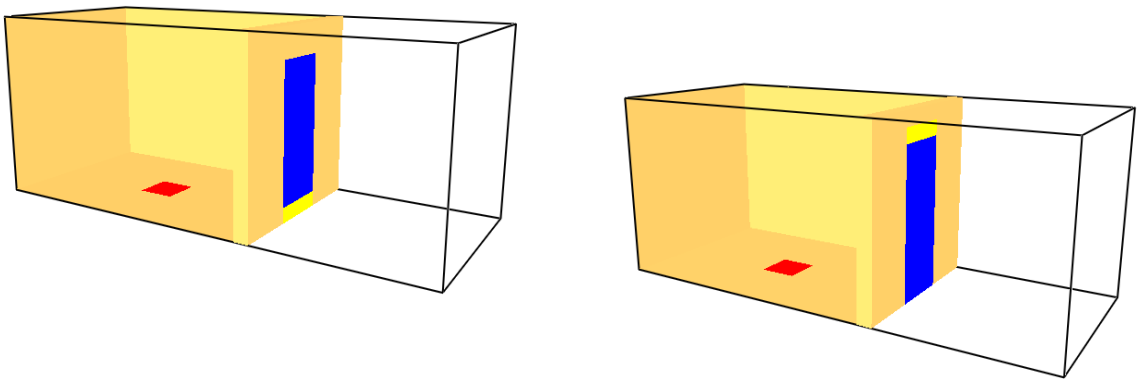

(a) (b)

Figure 2.3.1. ISO room configuration in FDS: (a) with leakage at the bottom; (b) with leakage at the top

2.3.3 Fire

100 kW fire with the size of 0.5 m x 0.5 m was selected, and n-heptane was assigned as the fuel.

2.3.4 Mesh resolution

Nominal cell size was calculated by using the characteristic diameter. According to Eq. (1), by taking into account heat release rate $\dot{Q}$ (kW),ambient density ρ_∞ (kg/m^3) and temperature T_∞ (K), gravity acceleration (m/s^2) and heat capacity of air c_p (J/kg.K), the cell size should be between 2.4 cm and 9.6 cm.

$$D^* = \left(\frac{\dot{Q}}{\rho_\infty T_\infty c_p \sqrt{g}}\right)^{2/5} \tag{2.9}$$

$$D^* = \left(\frac{100}{1.2 \times 293 \times 1 \times \sqrt{9.81}}\right)^{2/5} = 0.383\ m$$

$$4 < \frac{D^*}{\delta x} < 16$$

$$2.4\ cm < \delta x < 9.6\ cm$$

2.3.5 Scenarios

Pressure zone was defined in accordance with the ISO room dimensions, and the leak path was from the room, ZONE 1, to the ambient, ZONE 0. To compare two leakage modelling methods, 10 different scenarios were created and simulated as can been seen from Table 2.3. The parameters that were varied include location of leakage surfaces and LEAK_PRESSURE_EXPONENT, while the area of the leakage and the size were kept constant.

Table 2.3. Leakage study scenarios

Method	Location	Size (L x H)	Area (m^2)	Exponent
Bulk leakage	Bottom of the door	0.8 m x 0.2 m	0.001	0.5; 0.75; 1.0
	Top of the door	0.8 m x 0.2 m	0.001	0.5
	All surfaces	NA	0.001	0.5
	One wall	NA	0.001	0.5
Localized leakage	Bottom of the door	0.8 m x 0.2 m	0.001	0.5; 0.75; 1.0
	Top of the door	0.8 m x 0.2 m	0.001	0.5

2.3.6 Post-processing

2.3.6.1 Slice files

For visualisation purpose, pressure, temperature and velocity slice files were defined across the room. For the latter parameter, animated vector files were created to observe the leakage flow.

2.3.6.2 Devices

- Pressure

Defining pressure zone enabled to identify the background pressure, while the total or local pressure was measured by using the pressure devices placed on the leakage surface when leak was defined on the top and the bottom of the door.

- HVAC output

Leakage flow was measured by using HVAC output quantities, namely `VOLUME_DUCT_FLOW`. Since the ambient is considered as Zone 0 and the room was defined as Zone 1, the duct connecting two zones was named as `'LEAK 0 1'`. In addition, `'DUCT DENSITY'` was used to determine the density of the flow.

2.4 Mons experiments validation study

For the validation study, Tests 3 with deactivated fans and Test 4 and no ventilation (Table 2.1) were considered.

2.4.1 FDS version

Validation study was performed by using FDS 6.5.2 version, as in the current FDS 6.6.0 version a fault was found: `LEAK_PRESSURE_EXPONENT` had no effect on the pressure values.

2.4.2 Geometry

The internal dimensions of testing facility were recreated: 2.4 m x 12.2 m x 2.4 m. 0.2 m thick partition wall, separating the fire room and adjacent room was placed at y=4 m, thereby dividing the container into 2 rooms with length of 4 m and 8 m. The door is 0.8 m wide and 2.0 m high.

2.4.3 Fire source

Table 2.4 shows the summary of input data for fire source. As it can be seen, only the size and HRRPUA were different for two tests, while other parameters were not altered. In addition, the HRR was prescribed by using RAMP function.

Table 2.4. Summary of input for fire source

	Soot yield	CO yield	Formula	ΔH_c (kJ/kg)	Fire size	HRRPUA (kW/m^2)
Test 3	0.005	0.0015	CH_2O	14000	0.4 m x 0.4 m x 0.4 m	360
Test 4	0.005	0.0015	CH_2O	14000	0.6 m x 0.6 m x 0.5 m	280

Before using CH_2O, $C_{3.4}H_{6.2}O_{2.5}$ was inputted as chemical formula for the wood. However, it resulted in earlier extinction of the fire as Figure 2.4.1; therefore, inputted HRR curve was not

retrieved. In the master thesis of Piret-Gerard, CH_2O was assigned as chemical formula for wood in CFAST simulations by referring to the 2nd edition of SFPE by Tewarson. According to SFPE Handbook, wood has a chemical formula of $(CH_2O)_n$, chemical formulas differ slightly based on the type of wood. By performing preliminary simulations, it was found out that HRR curve is well captured by CH_2O.

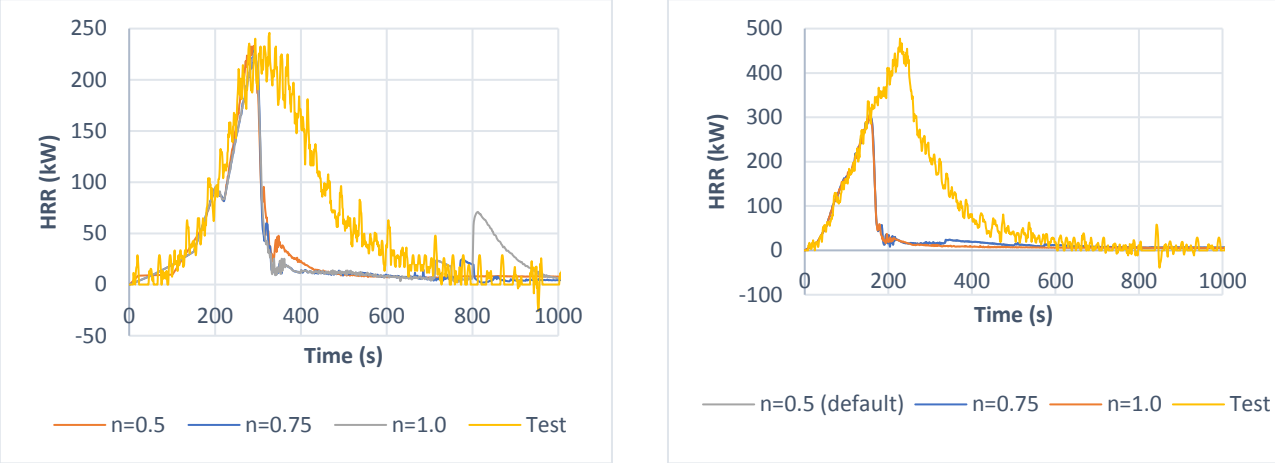

(a) Test 3 (b) Test 4

Figure 2.4.1. HRR with $C_{3.4}H_{6.2}O_{2.5}$

2.4.4 Mesh resolution

Nominal cell size was again calculated by using characteristic diameter concept based on the peak HRR. As a result, for Test 3 the cell size should be between 3.3 cm and 13.3 cm, while for Test 4 the range is between 4.7 cm and 19 cm. It was decided to perform sensitivity analysis with 5 cm and 10 cm mesh resolution in both cases.

2.4.5 Boundary conditions

As it has been mentioned before, the test facility has 0.2 m thick concrete walls, which are insulated with 0.05 m rockwool and two layers of 0.013 m thick plasterboard. The partition wall consists of two plasterboards with rockwool in between, while door consists of two steel layers and foam placed in between. The material properties used in the model are shown in Table 2.5. BACKING='EXPOSED' back side boundary condition was applied to estimate heat transfer through the wall.

Table 2.5. Thermal material properties

Material	Conductivity (W/m.K)	Specific heat (kJ/kg.K)	Density (kg/m^3)
Concrete	0.7	0.75	2200

Rockwool	0.035	0.84	45
Gypsum	0.48	0.84	1440
Steel	50.2	0.49	8050
Foam	0.028	1.45	800

2.4.6 Leakage modelling

Both leakage modelling approaches were implemented in the model. As part of the pressure zone leakage, two pressure zones were defined for each room since the door was closed during the experiments. `Zone 1` corresponds to the adjacent room, while `Zone 2` is assigned to the fire room. The total leakage area of 0.0026 m^2 was determined at 50 Pa overpressure by conducting the blower door test. Therefore, for the reference cases of Tests 3 and 4, the leak areas of 0.016 m^2 and 0.001 m^2 were prescribed to the fire room and the adjacent room, respectively. The surfaces within the pressure zones were defined as leaking by indicating `LEAK_PATH` to ambient which is Zone 0 by default. In addition, default values of `LEAK_PRESSURE_EXPONENT` (0.5) and `LEAK_REFERENCE_PRESSURE` (4 Pa) were kept for the reference cases.

Localized leakage approach was used to define the leak through a gap under the partition door dividing the fire and adjacent rooms. To achieve this, two `VENT`s were created on the door and connected by HVAC duct with area of 0.008 m^2.

2.4.7 Ventilation

During Test 3, the pipes were open, and fans were turned off. The ventilation in FDS was modelled with a circular HVAC duct with 100 mm diameter connected to the ambient. The lengths of the ducts connected to the fire room and the adjacent room were defined as 4.9 m and 4.1 m, respectively.

Since no detailed information about ventilation was provided, a number of assumptions were made. To illustrate, it was assumed that ducts are made of galvanized steel. As a result, roughness of 0.00015 m corresponding to average roughness was assigned to the duct connecting the fire room and ambient, whereas 0.00009 m corresponding to medium smooth roughness was selected for the duct connecting the adjacent room and the ambient. Losses in duct are based on wall friction and fittings. Wall friction losses are taken into account by inputting roughness, while pressure losses through fittings such as elbows, bends, and tees are considered by specifying $K_{fitting}$. The coefficient was estimated based on the Eq. (2.6) by assuming that the flow is steady-state and term

$\rho g \Delta z$ is negligible. Since the fans are deactivated, $\Delta p_j = 0$. Therefore, minor loss coefficient equals:

$$K_{fitting} = \frac{2\Delta p}{\rho u^2}$$

Based on the experimental measurements of pressure and volume flow rate in ducts, loss coefficients for both ducts were estimated as 11 and 20 for forward and reverse flows, respectively.

2.4.8 Post-processing

Devices were placed in accordance with the experiments:

- 11 temperature devices were installed in two locations every 0.2 m per room to recreate thermocouple trees.
- The surface temperature of a wall was measured every 60 cm by three temperature devices, and one was also placed behind the first layer of plasterboard.
- One more temperature device was placed right above the fuel source at 2.2 m height.
- Two devices with pressure quantity were also modelled in each room.
- To capture the flow rate through leaks and in ventilation ducts, a device with `'DUCT VOLUME FLOW'` command was implemented.
- To determine the oxygen level, devices measuring wet and dry oxygen were incorporated into the model.

2.4.9 Scenarios

To determine the importance of certain parameters, a number of scenarios were developed for each test. Table 2.6 lists the major variables and the corresponding input in FDS. It can be seen that parameters related to the pressure zone leakage modelling including leakage area, leak pressure exponent, and leak reference pressure were varied. Pressure zone area values were chosen arbitrarily by increasing the reference area of 0.0026 m^2 by 50% and 100%. Flow exponent values were selected based on the literature review: it was found to lie between 0.4-1.0 with 0.65 being used for normal buildings. Leak reference pressure was changed to 50 Pa because it corresponds to the pressure at which leakage area was measured during the blower door test. In addition, it was decided to study the influence of leak pressure exponent with 50 Pa reference pressure. For localized leakage, the location was changed from bottom of the door to the top. Also, the area of the aperture was arbitrarily increased to 0.012 m^2 (50%).

Table 2.6. FDS input variables

Parameter	Reference case	Variable
Pressure zone area	0.0026 m^2	0.0039 m^2
		0.0052 m^2
Leak pressure exponent	0.5	0.65, 0.75, 1.0
Leak reference pressure	4 Pa	50 Pa
Localized leakage area	0.008 m^2	0.0012 m^2
Location of localized leak	Bottom	Top

3. Results

3.1 Leakage modelling study

3.1.1 Mesh sensitivity

For mesh sensitivity analysis, the cell size of 5 and 10 cm were used, and the main parameters such as pressure and leakage flow are compared for leakage modelling methods. In both cases, slightly higher pressures and leakage flows are obtained with finer mesh in decay phase. Nevertheless, the discrepancy is not significant; thus, the coarse mesh of 10 cm will be used to decrease computational time.

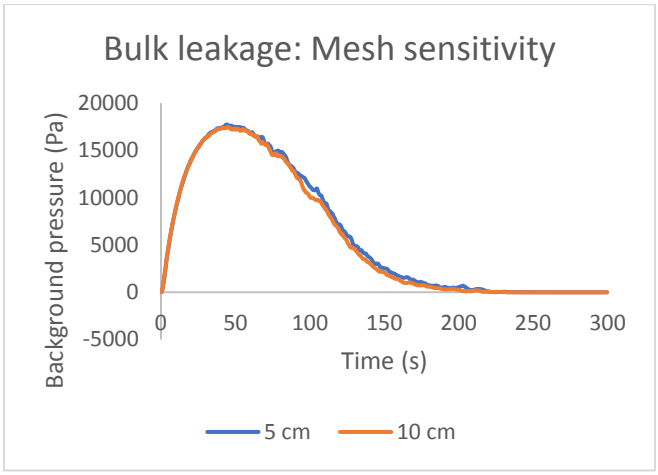

(a) Background pressure

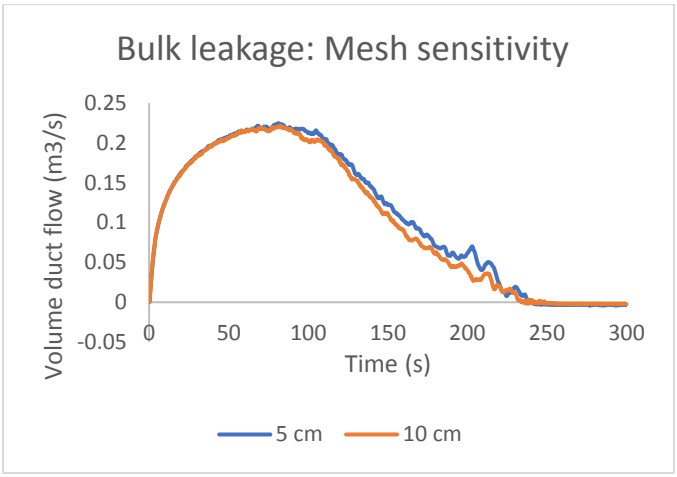

(b) Leakage flow

Figure 3.1.1 Bulk leakage mesh sensitivity

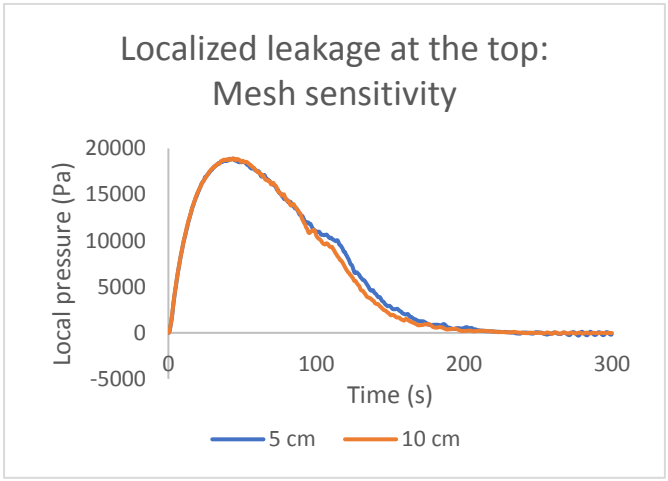

(a) Local pressure

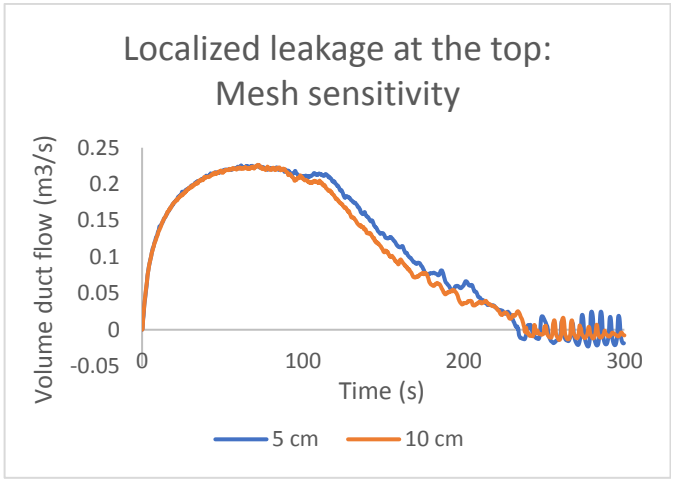

(b) Leakage flow

Figure 3.1.2. Localized leakage mesh sensitivity

3.1.2 Bulk leakage and Localized leakage

The results of two leakage modelling methods with the leak at the bottom and at the top of the door are compared in the following graphs. By comparing corresponding local and background pressure profiles, the deviations of up to only 7% were obtained. Figure 3.1.3 also show that higher values of pressure were obtained when Localized leakage approach was used. To illustrate, the peak pressures of 20 kPa and 19 kPa were obtained with Localized leakage at the bottom and top of the door, respectively. Changing leakage location resulted in different tendency for two approaches: for Localized leakage overpressure was higher with leak at the bottom, whereas leak at the top resulted in higher pressures with Bulk leakage.

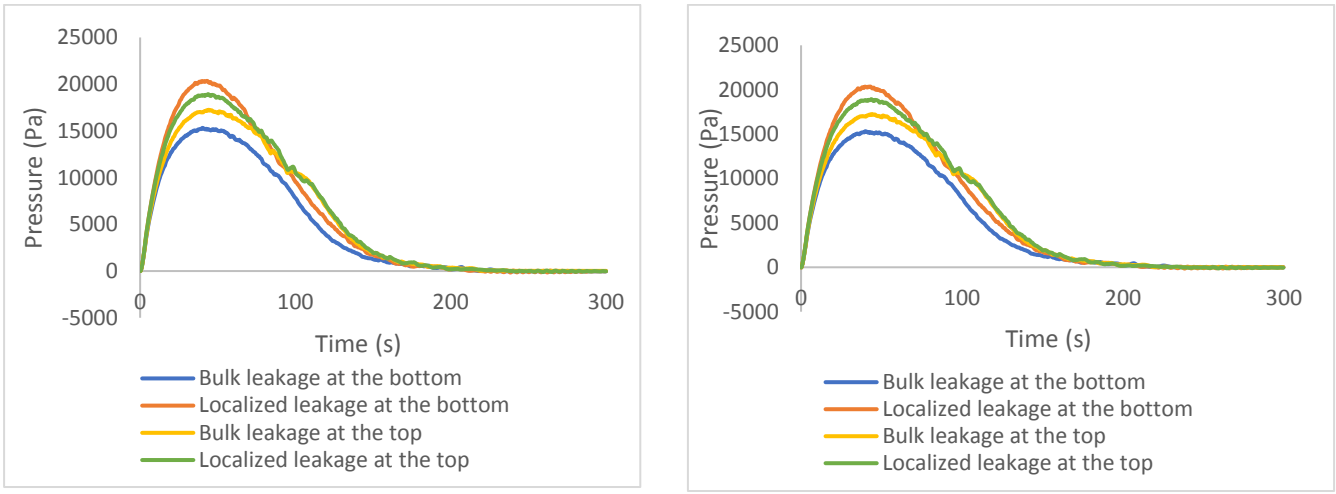

(a) Local pressure profile

(b) Background pressure profile

Figure 3.1.3. Comparison of local and background pressures

As Figure 3.1.4 shows the peak leakage flow is 0.225 m^3/s for Localized leakage, while the lowest leakage flow of 0.208 m^3/s is obtained for Bulk leakage at the bottom of the door. Generally, it can be seen that leakage flow rate profiles do not differ much apart from the Bulk leakage at the bottom of the door. It should be noted that for Bulk leakage method leakage flow was expressed as leak from the ambient to the 'Zone 1' with negative sign; thus, the sign was adjusted to compare the results.

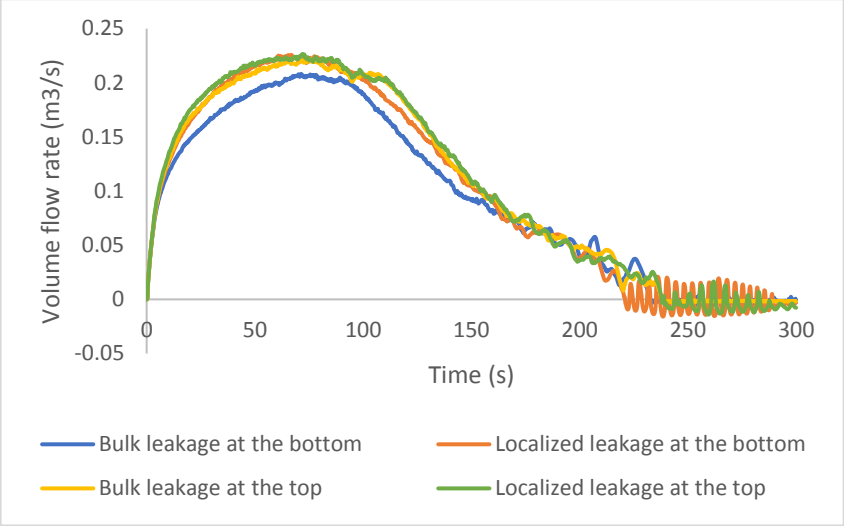

Figure 3.1.4. Leakage flow profile

3.1.3 Bulk leakage

Relocating the leak from the bottom and to the top of the door for bulk leakage resulted in higher local and background pressures along with higher leakage flow rate as Figure 3.1.3 and Figure 3.1.4 illustrate. For the leakage at the top, pressure increased up to 17 kPa, while 15 kPa was the peak for the leakage at the bottom. The maximum flow rate was about 0.222 m^3/s for the leak at the top and 0.208 m^3/s for the case with the bottom leak.

In Figure 3.1.5a, background pressure and leakage flow rate are plot in one graph for Bulk leakage at the bottom of the door, and it can be seen that the pressure peak is followed by the peak in leakage flow. Therefore, increase in pressure brings about rise in leakage flow but with a time delay of about 30 s. Regarding the leak at the top, the same tendency is observed; however, the time delay is less compared to the case with the leak at the bottom.

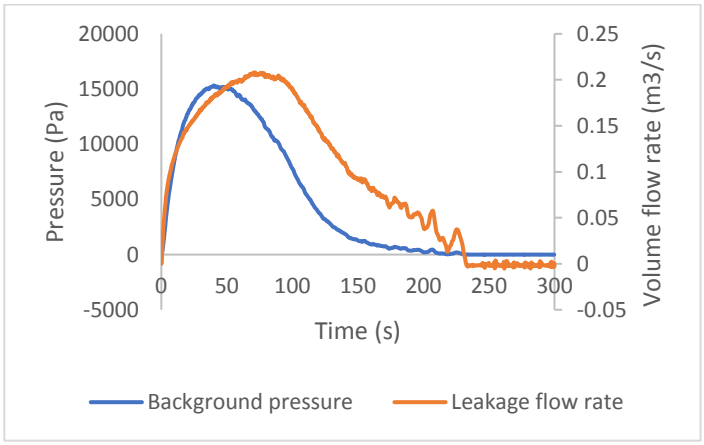

(a) Bulk leakage at the bottom

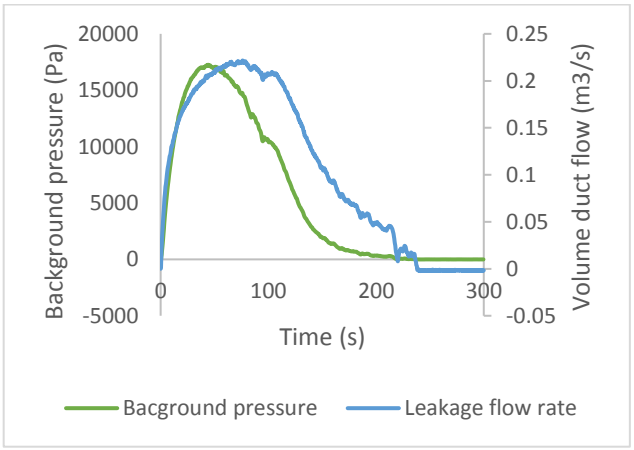

(b) Bulk leakage at the top

Figure 3.1.5. Background pressure and leakage flow rate

As Bulk leakage method is usually used when the location of leakage is not known, more simulations were performed by defining all surfaces and front wall as leakage paths. By comparing background pressure profiles in Figure 3.1.6, it can be seen that the lowest profile is obtained when the leak is at the bottom of the door, while higher background pressures were observed when leakage was defined through all surfaces and at the top of the door. It should be noted that the background pressure profiles in latter two cases are almost identical.

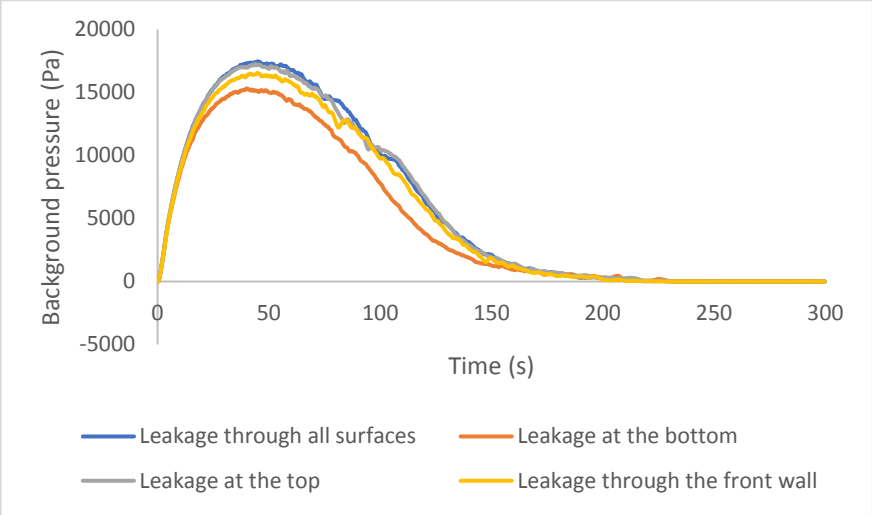

Figure 3.1.6. Background pressure: bulk leakage with different leakage paths

By comparing leakage flows from different scenarios of Bulk leakage, the it can be observed that volume flow rate profiles of leakage through all surfaces and leakage at the top are similar (Figure 3.1.7). The peak of about 0.217 m^3/s is obtained for leakage through all surfaces. When the leak path was defined at the bottom of the door, the leakage flow rate was the lowest. The positive relation between background pressure and leakage flow with leak at the bottom of the door can be noticed from two graphs on Figure 3.1.6 and Figure 3.1.7.

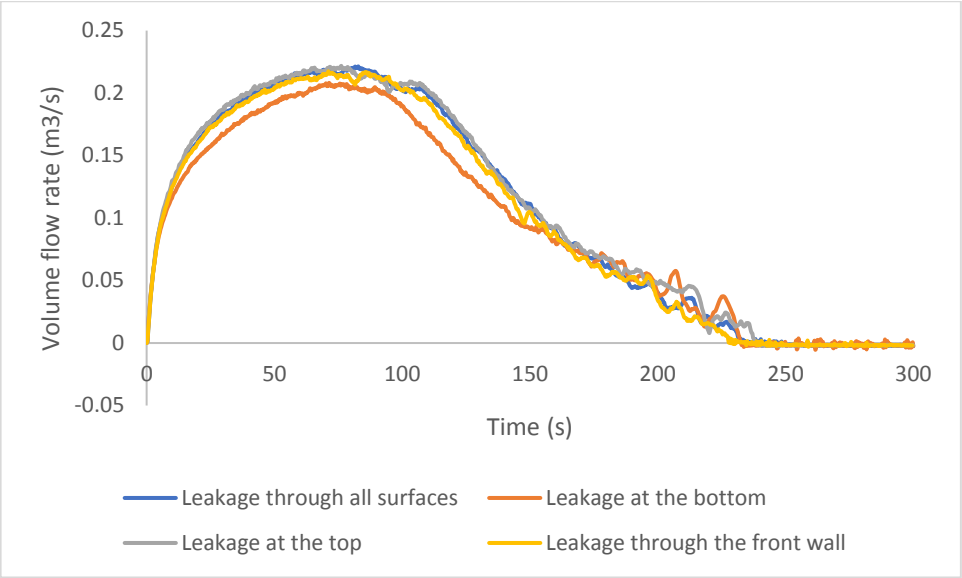

Figure 3.1.7. Leakage flow: bulk leakage with different leakage paths

3.1.4 Localized leakage

The location of the leak either on the top or bottom of the door affects the parameters such as volumetric leakage flow rate, local and background pressures. When leakage is defined at the bottom higher value of peak pressure is obtained in comparison with leakage at the top of the door: around 20 kPa and 19 kPa, respectively. According to Figure 3.1.4, volumetric leakage flow rate was up to 7% higher for the leakage at the top. In this case, the correlation between pressure and volumetric leakage flow rate can be seen: lower leak flow to the ambient results in higher pressures and vice versa.

By plotting pressures on the same graph as leakage flow, similar behaviour as in Bulk leakage can be observed: rise in pressure causes increase in leakage flow, but with a time delay. To illustrate, the maximum local pressure of 19 kPa occurred at 43 s, and at 72 s peak leakage of 226 m^3/s is detected. Pressure drop is also followed by the decrease in leakage flows.

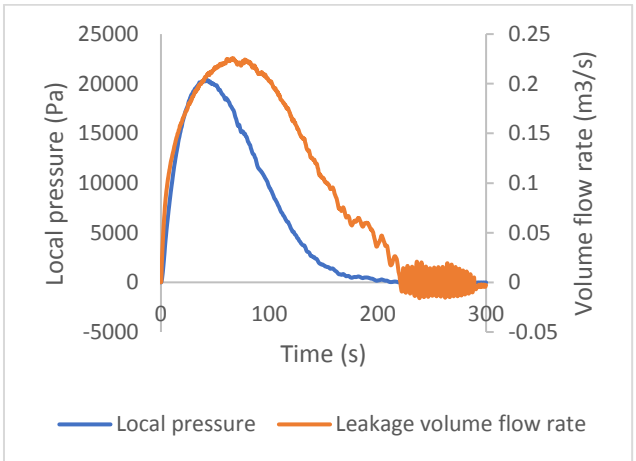

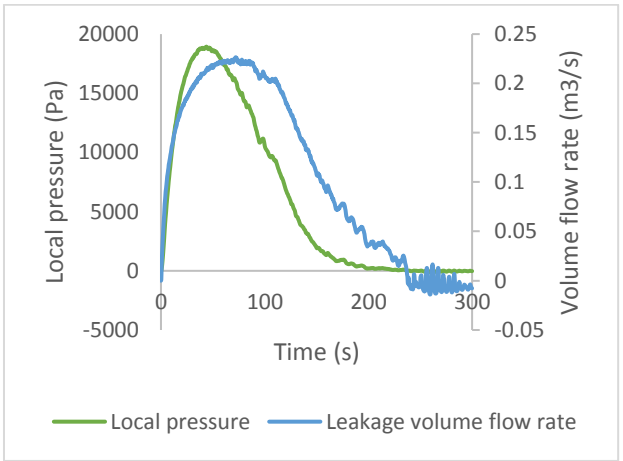

(a) Localized leakage at the bottom (b) Localized leakage at the top

Figure 3.1.8. Local pressure and leakage volume flow rate

3.1.5 Leak pressure exponent

`LEAK_PRESSURE_EXPONENT` is the parameter of pressure zone leakage, and it is 0.5 by the default in FDS. Figure 3.1.9 shows that changing the default value of `LEAK_PRESSURE_EXPONENT` considerably affects the pressure development: increase in the exponent leads to lower pressure in enclosure. With the default value the highest value of background pressure is 17 kPa. 1441 Pa is the peak pressure corresponding to 0.75 exponent, while maximum of 341 Pa is obtained when the exponent was changed to 1.0. This might be explained by the fact that leak area changes with pressure when the default exponent value is changed as indicated in Eq.(2.8).

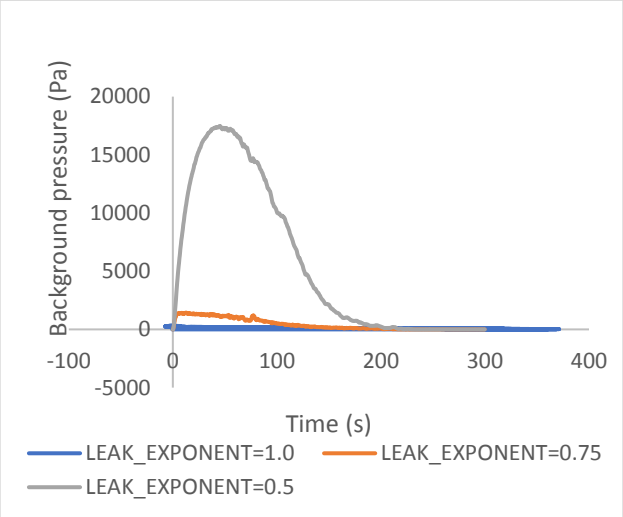

Figure 3.1.9. Effect of the exponent on the background pressure

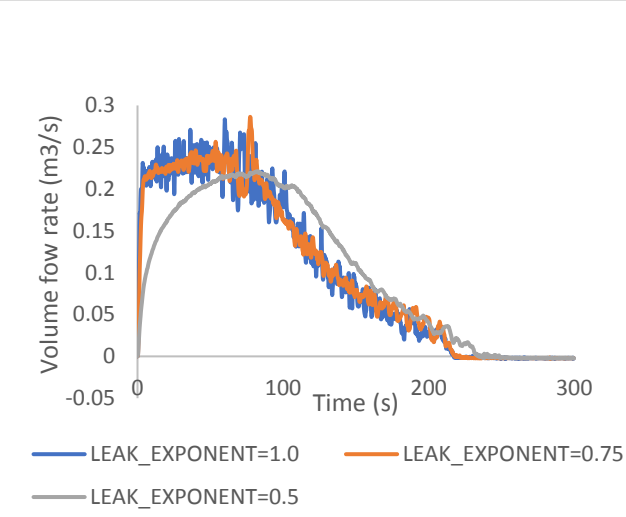

Figure 3.1.10. Effect of the exponent on the leakage flow

3.1.6 Verification of volume flow rate

By using output data, namely `'DUCT DENSITY'` and background pressure, the volume flow rate through leakage was calculated by using Eq. (2.7) and compared with post-processed `'VOLUME DUCT FLOW'`. Moreover, leakage flow was also estimated by using the ambient density. As can be seen from the graphs, using measured flow density better approximates the post-processed volume flow compared to ambient density.

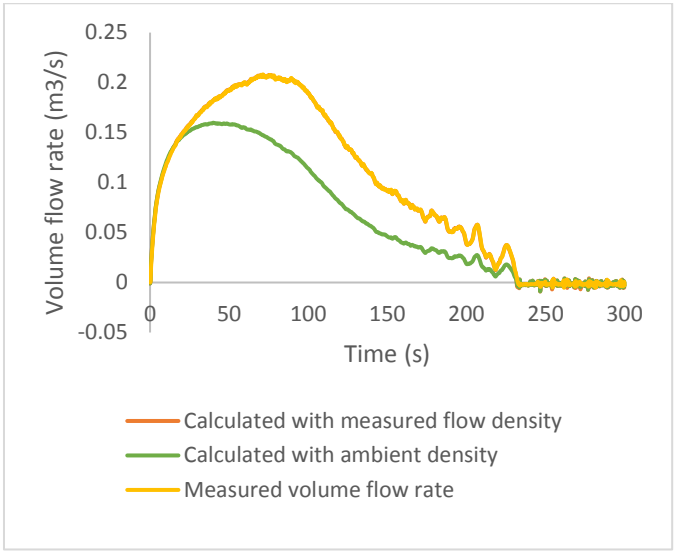

(a) Bulk leakage at the bottom

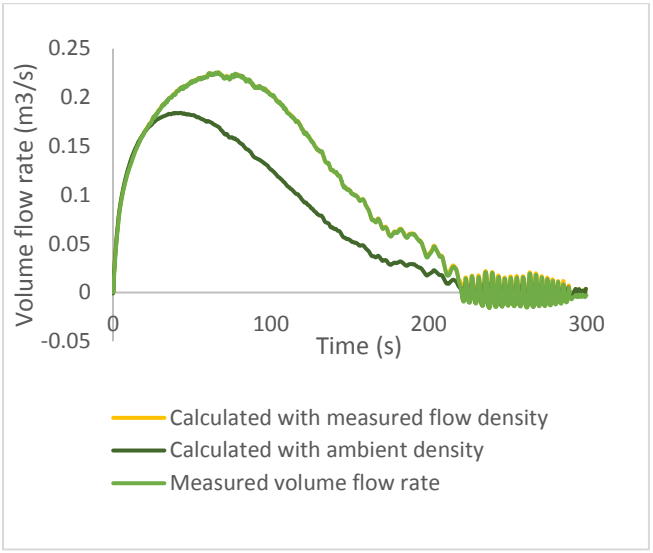

(b) Localized leakage at the bottom

Figure 3.1.11. Verification of volume flow rate

3.2 Test 3

3.2.1 Mesh sensitivity

By comparing the pressure profile in fire room obtained with 5 cm and 10 cm cells presented in Figure 3.2.1a, deviation during the pressure rise can be seen: finer cells give up to 10% lower pressure values. Volume flow rate profile do not change significantly. Despite this deviation, it was decided to adopt 10 cm mesh to decrease computation time.

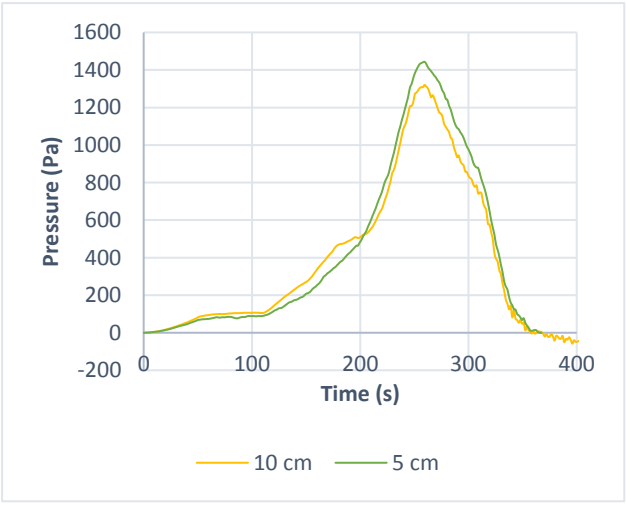

(a) Pressure in fire room

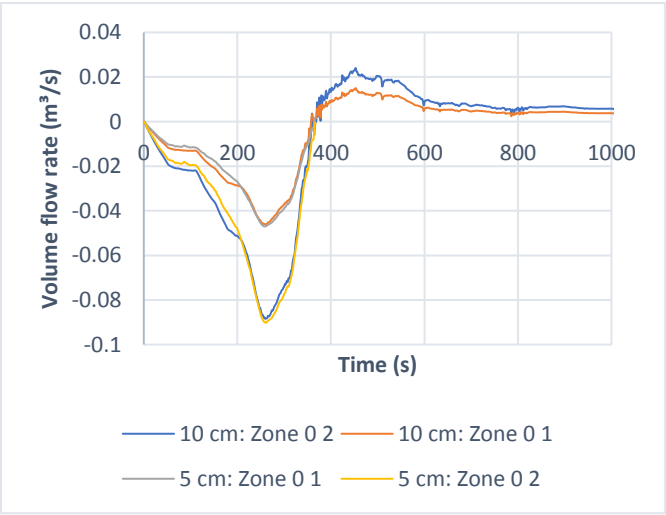

(b) Bulk leakage volume flow rate

Figure 3.2.1. Mesh sensitivity Test 3

3.2.2 HRR

As HRR is one of the most important parameters of the fire, the values should be checked to see if it corresponds to the imposed HRR. Figure 3.2.2 presents HRR graphs obtained by using the chemical formula of CH_2O, and it can be seen that there is a good agreement between experimental and CFD results. The peak HRR of 224 kW was obtained in FDS model as was prescribed based on the available experimental data.

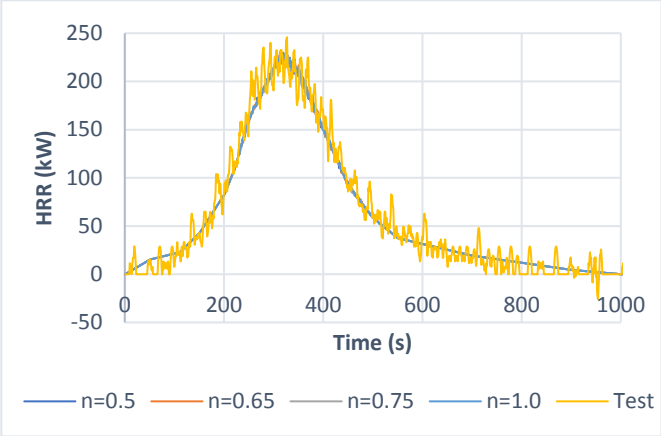

(a) $p_{ref} = 4\ Pa$ and varied exponent

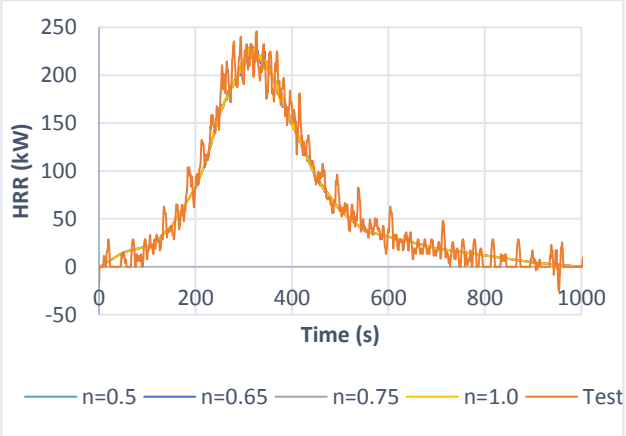

(b) $p_{ref} = 50\ Pa$ and varied exponent

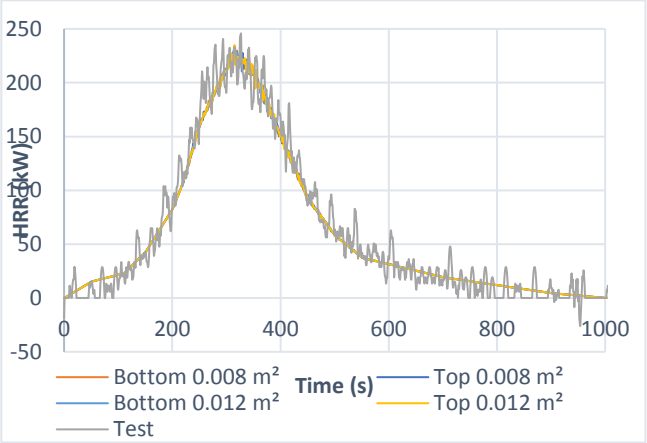

(c) Localized leakage location and area

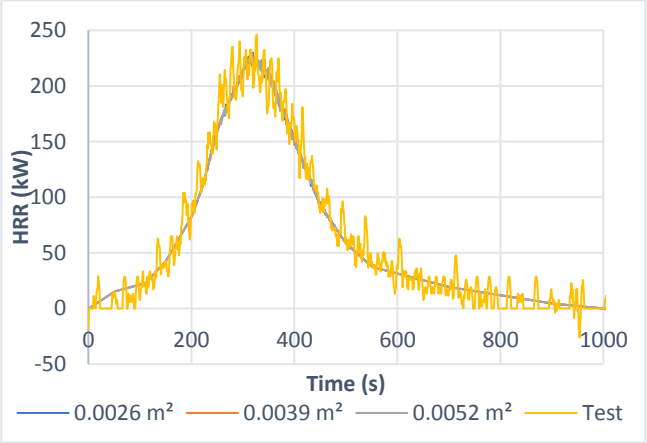

(d) Bulk leakage area

Figure 3.2.2. Comparisons of HRR (Test 3)

3.2.3 Pressure

By looking at the pressure graphs in fire room, for the reference case, which corresponds to the leak exponent being equal to 0.5, FDS significantly overestimates the overpressure with peak of around 1300 Pa, while during the test peak of 270 Pa was measured. This might be caused by assigning a constant leak area based on the blower door test. However, pressure during fire reaches much higher values in comparison to imposed overpressure by conducting blower door test. Therefore, by introducing `LEAK_PRESSURE_EXPONENT`, the change in leakage area with pressure during fire is considered. As Figure 3.2.3a and Figure 3.2.3b show pressure values

decrease as default exponent is changed. It can be also seen that experimental pressure profile is captured better when $n = 0.75$ with $p_{ref} = 4\ Pa$, while for the case with $p_{ref} = 50\ Pa$, changing exponent value did not result in accurate prediction of experimental pressure profile as even the maximum value $n = 1.0$ slightly overestimates the overpressure. Thus, reference pressure value affects the leakage area: increase in reference pressure leads to lower pressure ratio ($\Delta p/p_{ref}$) in Eq.(2.8), thereby increasing exponent value required to match the experimental data.

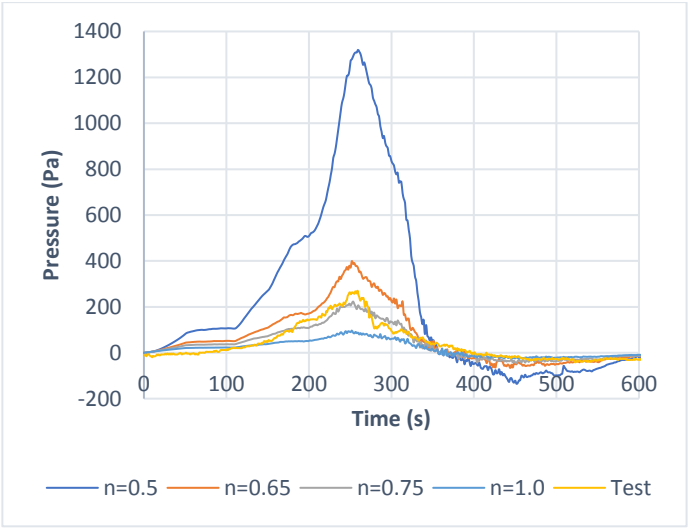

(a) $p_{ref} = 4\ Pa$ and varied exponent

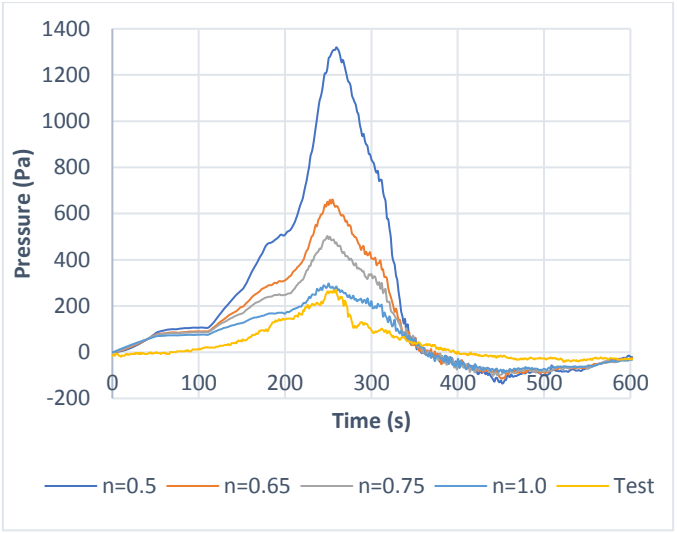

(b) $p_{ref} = 50\ Pa$ and varied exponent

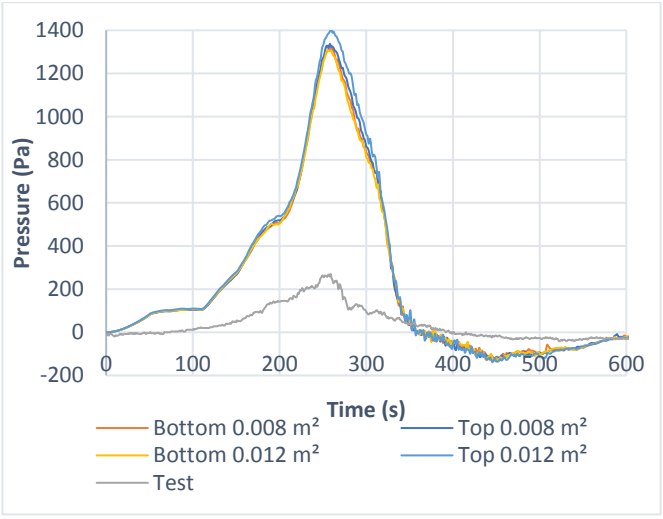

(c) Localized leakage location and area

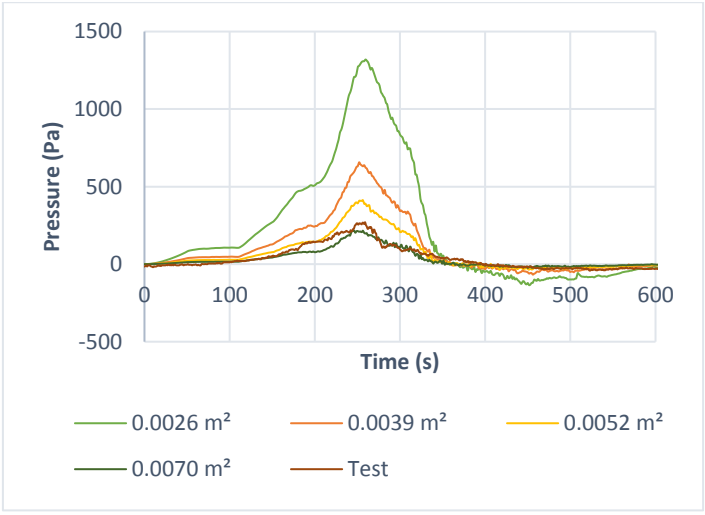

(d) Bulk leakage area

Figure 3.2.3 Comparison of pressure profile in fire room (Test 3)

Location and area of the localized leak Regarding bulk leakage area, arbitrarily increased bulk leakage areas overpredicted the pressure in fire room. Additional simulation with total leak area of 0.0070 m^2 (0.0044 m^2 in fire room) resulted in lower pressure values compared to the experimental.

shows the comparison of pressure difference between fire room and adjacent room. During the experiment, the pressure difference between room was up to 7 Pa only. By comparing the results, the pressure difference measured during the test is lower compared to the pressure difference obtained via FDS simulations: with FDS the peak pressure of around 25 Pa has been obtained. Results also show that pressure exponent nor reference pressure do not have a significant impact on the pressure difference profile obtained except in case with $n = 1.0$ with $p_{ref} = 4\ Pa$ where the peak pressure is lower compared to other scenarios. **Error! Reference source not found.**c shows that when the localized leak area between two rooms is enlarged, the pressure difference between two rooms decreases. In addition, changing the location of the localized leak has an impact on the pressure difference, as with the leak at the top lower pressure difference is observed.

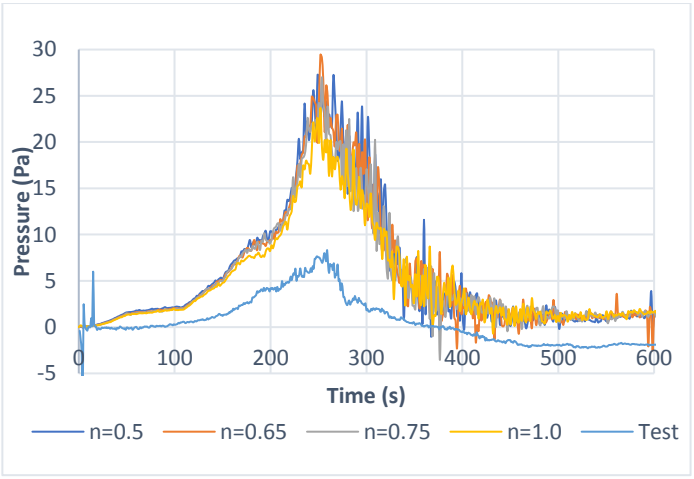

(a) $p_{ref} = 4\ Pa$ and varied exponent

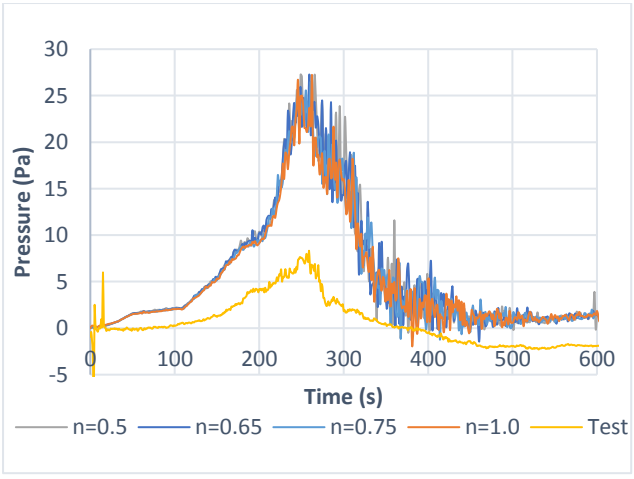

(b) $p_{ref} = 50\ Pa$ and varied exponent

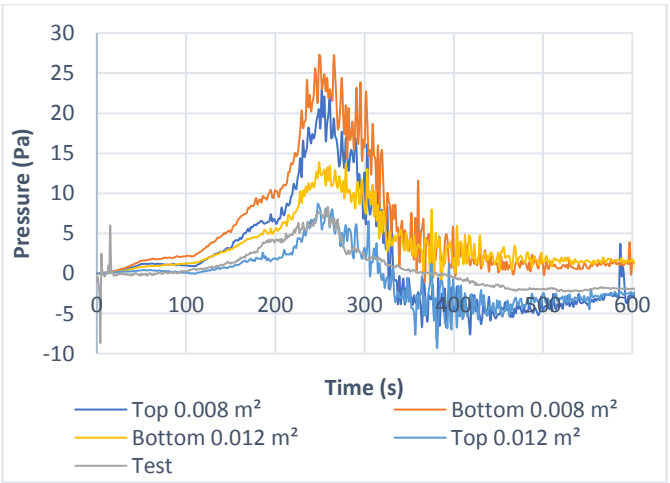

(c) Localized leakage location and area

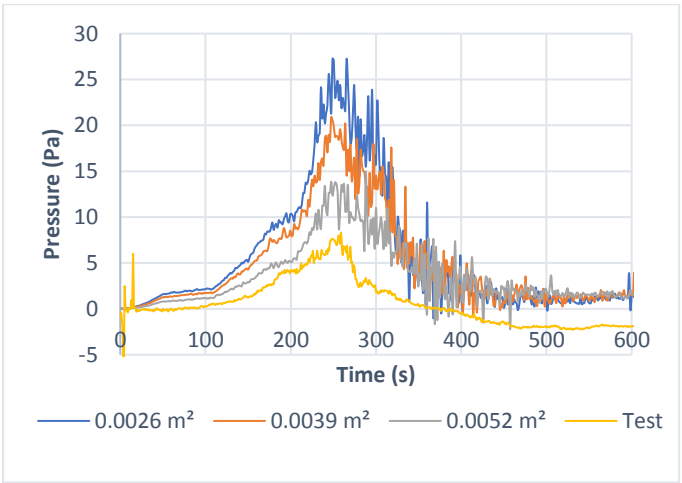

(d) Bulk leakage area

Figure 3.2.4. Comparison of pressure difference between two rooms (Test 3)

3.2.4 Leakage volume flow rate

By looking at the volume flow rates through pressure zone leak with default reference pressure, it can be seen that volumetric flow rate through leaks in adjacent room is slightly reduced with rising the exponent value. On the contrary, moderately higher flow rate out of fire room (`Zone 2`) during overpressure is observed due to increased exponent: 0.105 m^3/s with $n = 0.5$ to 0.091 m^3/s with $n = 1.0$.

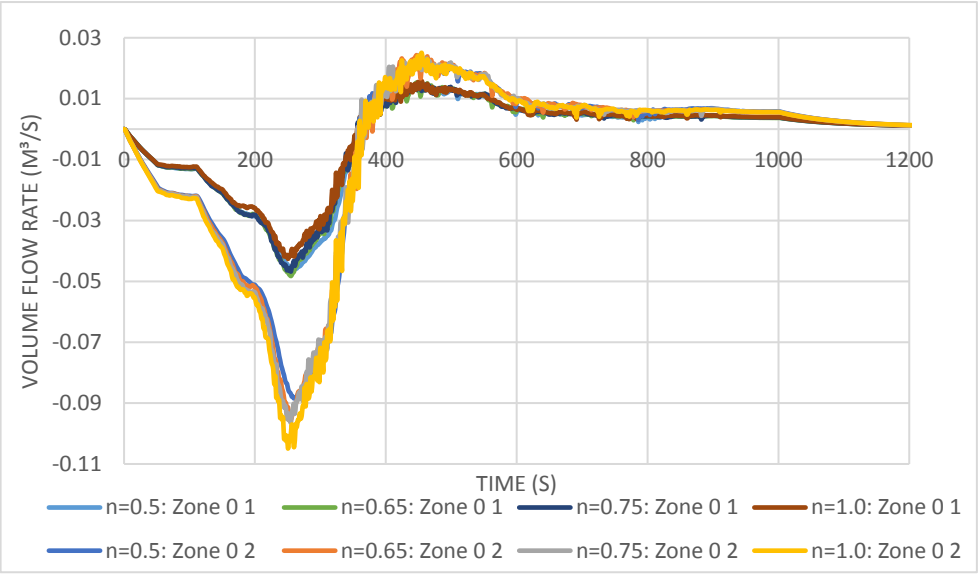

Figure 3.2.5 Comparison of volume flow rate through bulk leakage with $p_{ref} = 4\ Pa$ (Test 3)

Figure 3.2.6 shows that when $p_{ref} = 50\ Pa$, similar trend is observed as for the default reference pressure, but to a less extent.

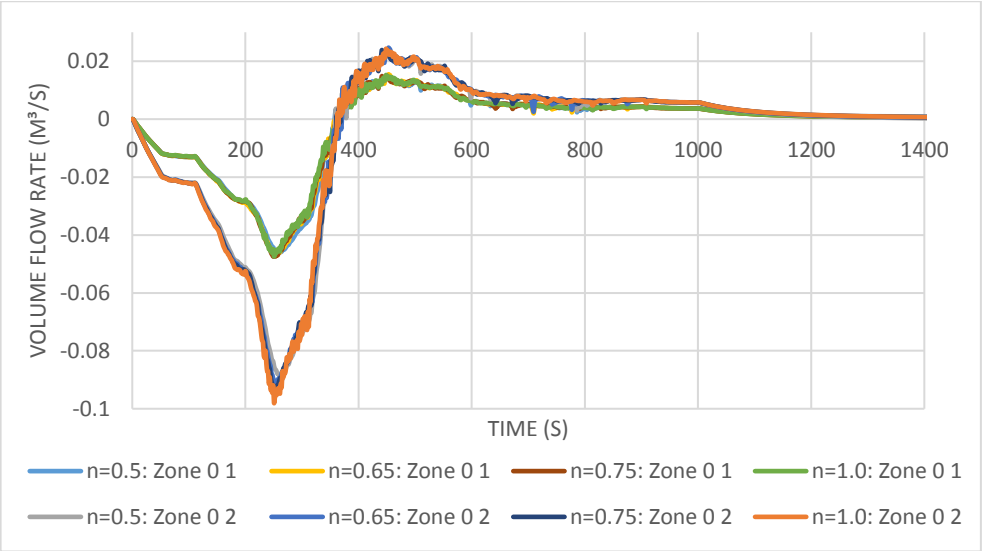

Figure 3.2.6 Comparison of volume flow rate through bulk leakage with $p_{ref} = 50\ Pa$ (Test 3)

As predicted, volume flow rate changes more significantly compared to the other cases when constant bulk leakage is increased. As can be seen from Figure 3.2.7, assigning larger constant area of bulk leakage brings about increase in flow rate out of the fire room during overpressure; however, it has an opposite effect for leakage from adjacent room.

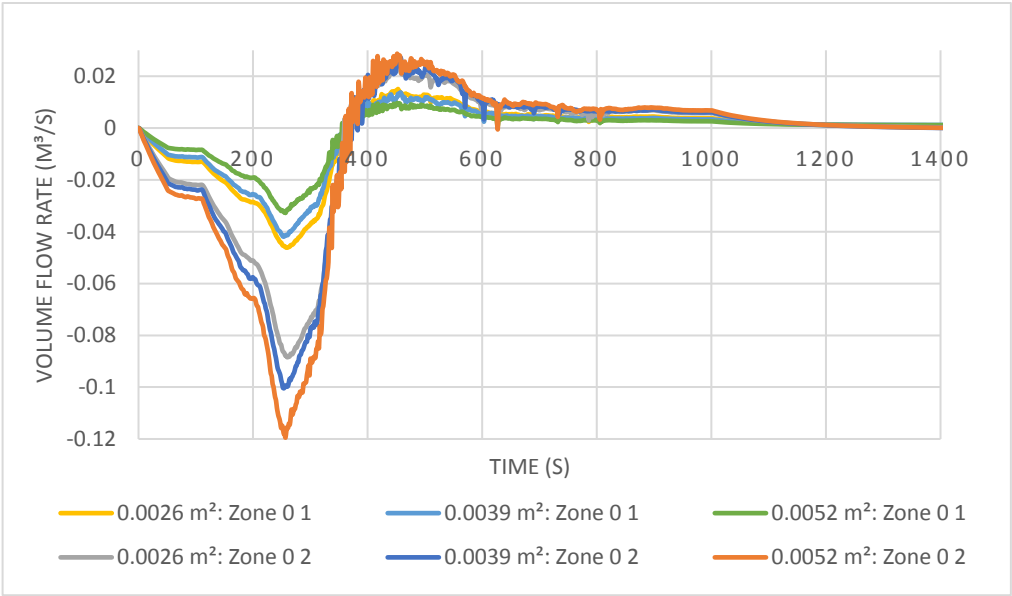

Figure 3.2.7 Comparison of volume flow rate through bulk leakage with varied bulk area (Test 3)

By comparing leakage flow rate between the fire room and adjacent room presented in Figure 3.2.8, it can be observed that it is slightly affected by the exponent value with the $p_{ref} = 4\ Pa$, while for $p_{ref} = 50\ Pa$ there is no substantial effect of varied exponent. Moderate increase in volume flow rate is remarked for localized leak at the top of the door, while no change was

observed when the localized leak area was enlarged. Increase of bulk leakage area also resulted in lower flow rate between two rooms through localized leak.

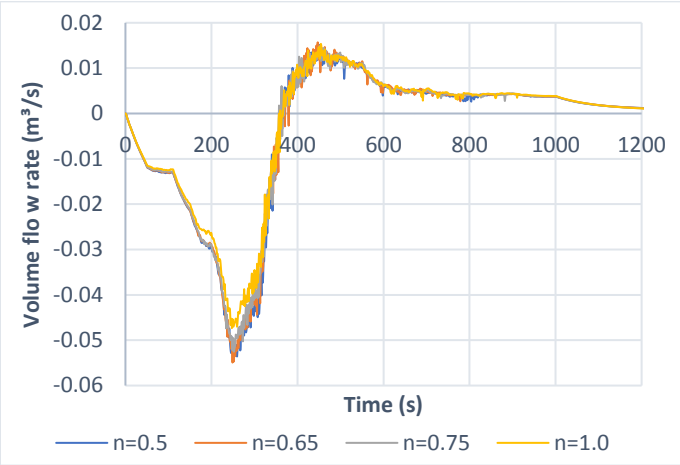

(a) $p_{ref} = 4\ Pa$ and varied exponent

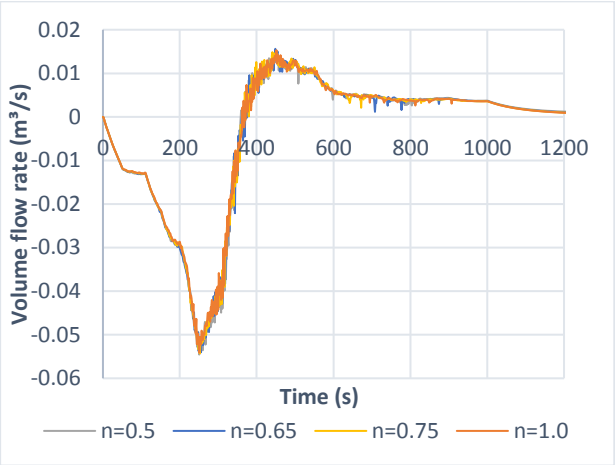

(b) $p_{ref} = 50\ Pa$ and varied exponent

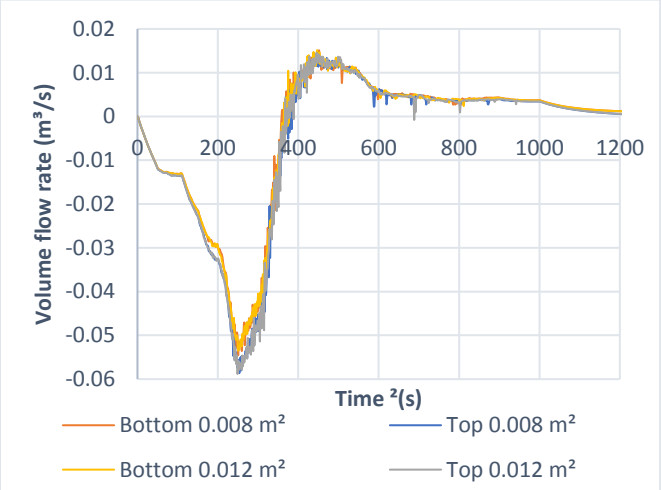

(c) Localized leakage location and area

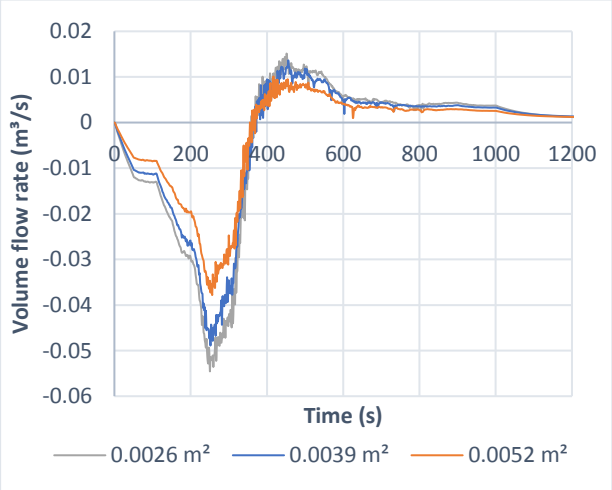

(d) Bulk leakage area

Figure 3.2.8 Comparison of volume flow rate through localized leakage (Test 3)

Considerably low volume flow rates in the ducts were obtained by FDS model as can be seen from Figure 3.2.9. It has been suggested that issue with the pressure solver is the reason for the obtained results; thus, `VELOCITY_TOLERANCE` was tightened and `MAX_PRESSURE_ITERATIONS` was increased to 50. However, it did not improve the results of volume flow rate through ducts. Another modification to the model was introduced: the mesh was aligned with the room geometry and the obstructions were changed to `VENTS` to reduce the velocity error at the walls. Nevertheless, it also did not contribute to the better match of volume flow with test measurements. Finally, setting mesh dimensions similar to the interior surface of the enclosure resulted in higher volume flow rate via ducts.

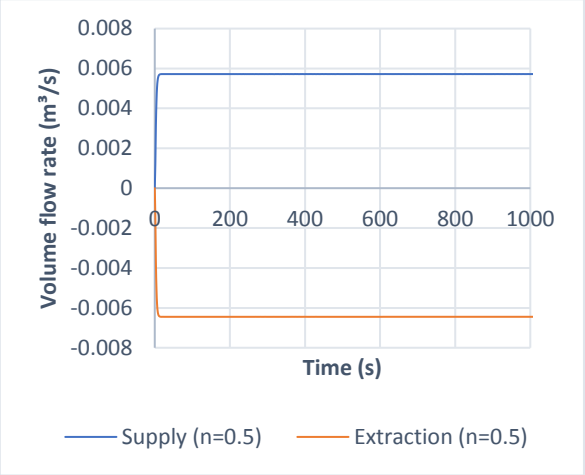

(a) FDS model

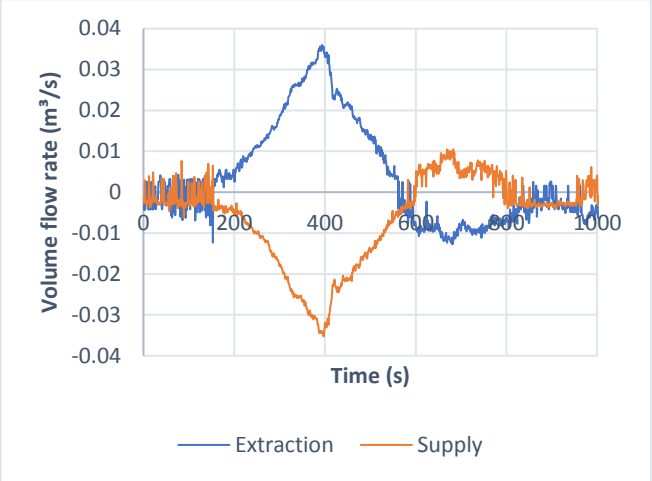

(b) Experiment

Figure 3.2.9 Comparison of flow rate in ducts

As Figure 3.2.10 shows that the adjusted model underpredicts the peak overpressure in the fire room by approximately 60 Pa due to slightly higher volume flow rate via ducts during overpressure. This discrepancy can be caused due to loss coefficients values specified as there is an inherent uncertainty as detailed ventilation system data was not available. It can be seen that supply duct in fire room acts as an exhaust during the overpressure, and in FDS it switches to supply earlier than during the experiment. Overpressure facilitates extraction for the exhaust as well, and similar pattern for the exhaust switching to supply in adjacent room can also be observed. As in the previous case, the pressure difference is overestimated by the FDS model. It should be noted that flow to adjacent room through localized leak is higher than flow out via bulk area in two rooms.

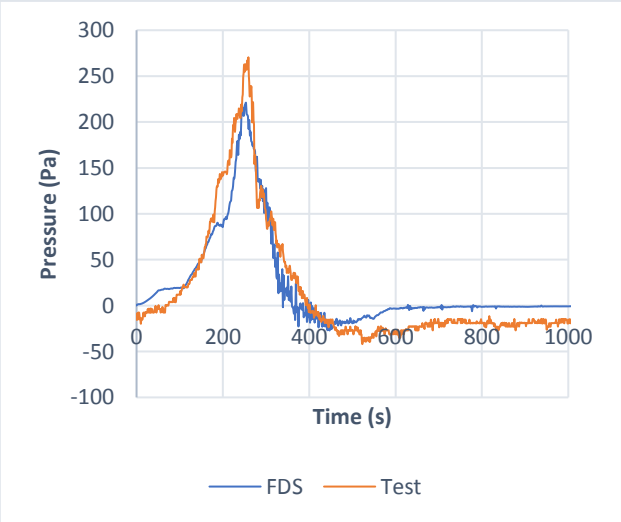

(a) Pressure development

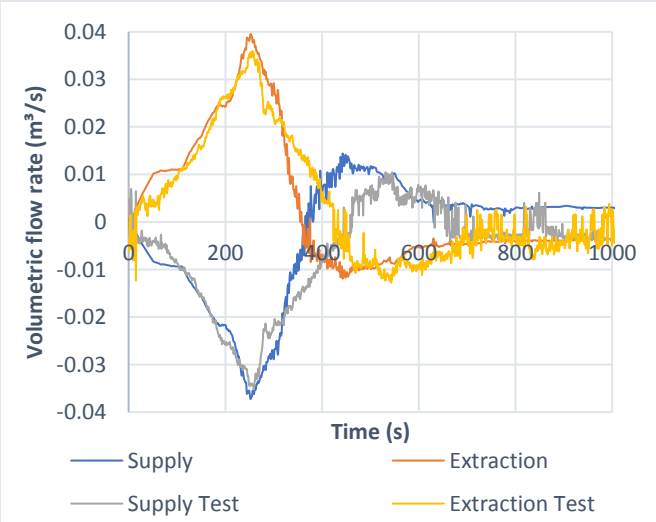

(b) Volume flow rate through ducts

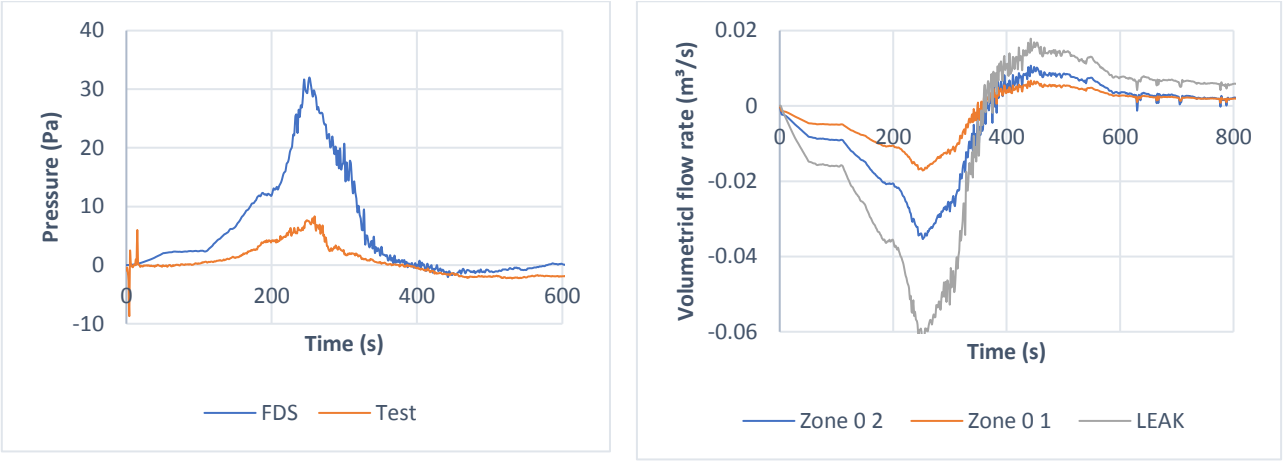

Figure 3.2.10. Adjusted model results

3.3 Test 4

3.3.1 Mesh sensitivity

By comparing the pressure profile in fire room obtained with 5 cm and 10 cm cells presented in Figure 3.3.1a, deviation during the pressure rise can be seen: finer cells give up to 20% lower pressure values, which results in up to 10% less volume flow rate during overpressure. Despite this deviation, it was decided to adopt 10 cm mesh to decrease computation time.

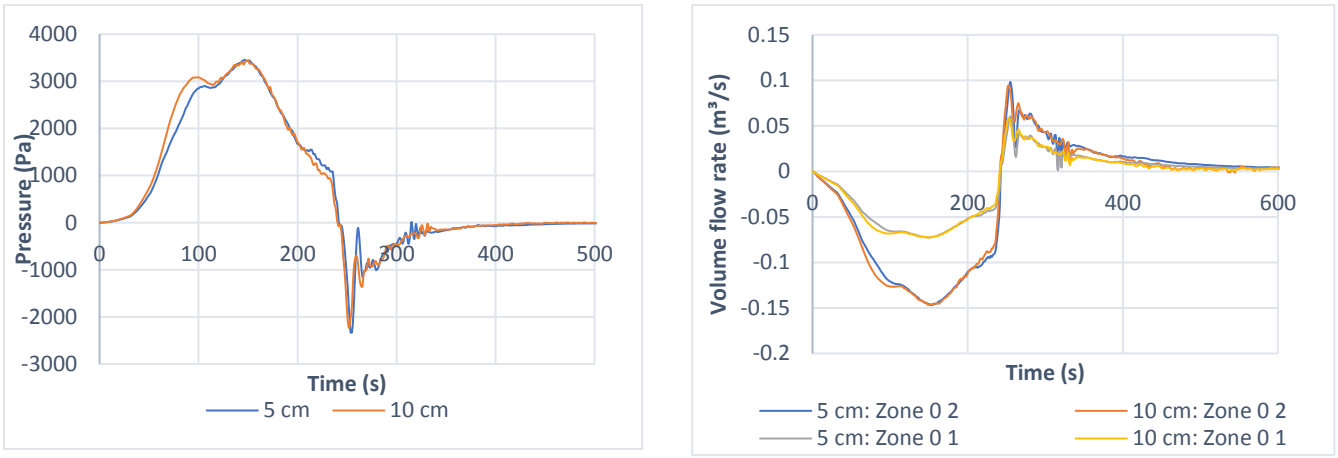

(a) Pressure in fire room (b) Bulk leakage volume flow rate

Figure 3.3.1.Mesh sensitivity results

3.3.2 HRR

By comparing the experimental and modelled HRR curves, presented in Figure 3.3.2, it can be seen that there is a deviation during the decay stage which is likely to develop due to lack of oxygen in fire room. Apart from that obtained peak HRR closely resembles the experimental peak of 455 kW.

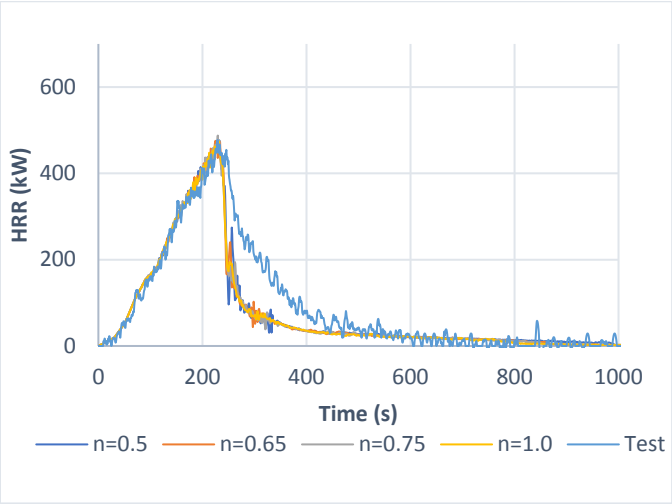

(a) $p_{ref} = 4\ Pa$ and varied exponent

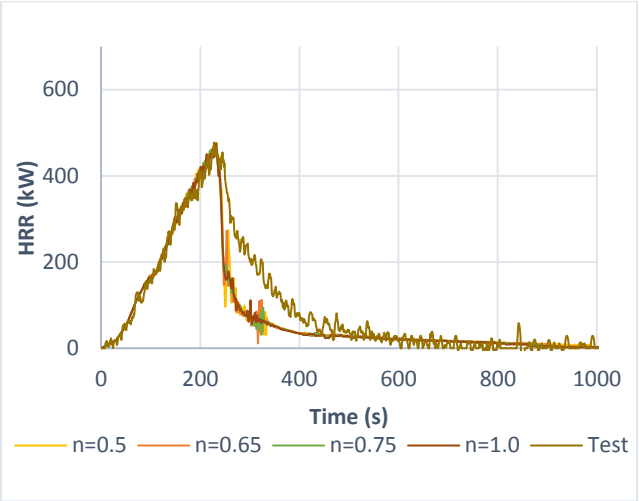

(a) $p_{ref} = 50\ Pa$ and varied exponent

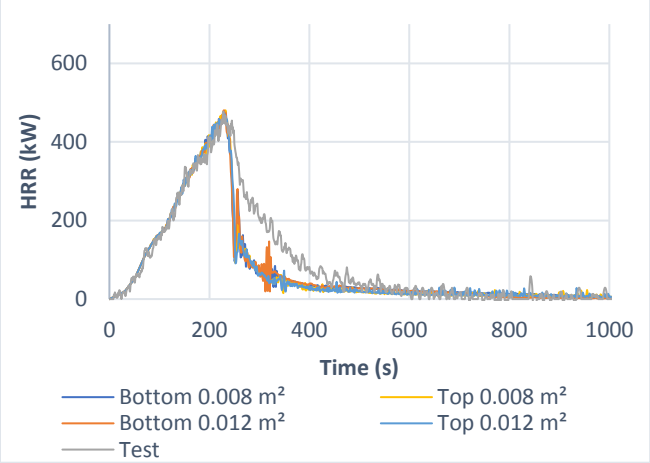

(b) Localized leakage location and area

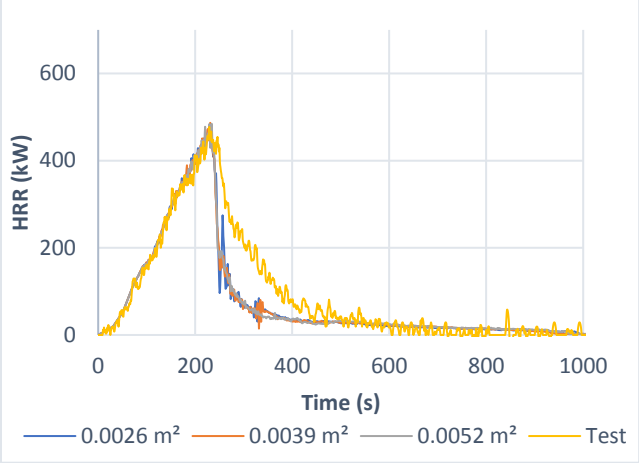

(c) Bulk leakage area

Figure 3.3.2. Comparison of HRR (Test 4)

To check whether oxygen deficiency causes the difference in the HRR profile, the oxygen measurements are checked. As Figure 3.3.3 reveals the oxygen in the room drops to 9% at around 255 s, and no combustion can be sustained any longer. Since the enclosure is airtight, flames are eventually extinguished by the descending hot layer at the ceiling. Air entrained into the plume will have less oxygen, thereby resulting in extinction of the fire. Therefore, energy release rate decreases faster and incomplete combustion takes place.

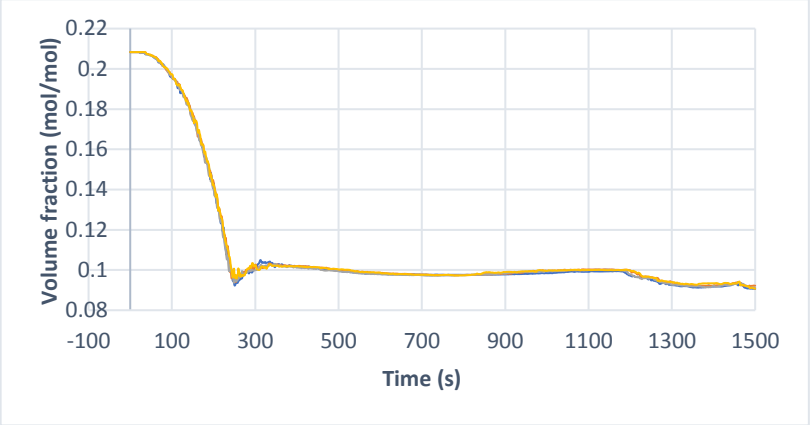

Figure 3.3.3. Oxygen consumption in fire room

3.3.3 Pressure

By comparing the pressure development in fire room, the same tendency of overprediction of overpressure by the reference case can be noticed: 1000 Pa was measured during the test, while 3300 Pa was obtained by FDS model. Thus, it can be stated that leakage area is larger than the prescribed value of 0.0026 m^2 by conducting blower door test. Figure 3.3.4 demonstrates that by employing the exponent parameter of 0.6, simulated pressure profile resembles the experimental for $p_{ref} = 4\ Pa$. For $p_{ref} = 50\ Pa$, the overpressure was captured with $n = 0.7$. Increase in the area of localized leak has not affected the pressure development considerably, whereas changing the location to the top has brought about up to 200 Pa higher peak pressure (Figure 3.3.4c). Regarding the bulk leakage, setting pressure zone leakage area to 0.0046 m^2 results in better match with the experimental overpressure.

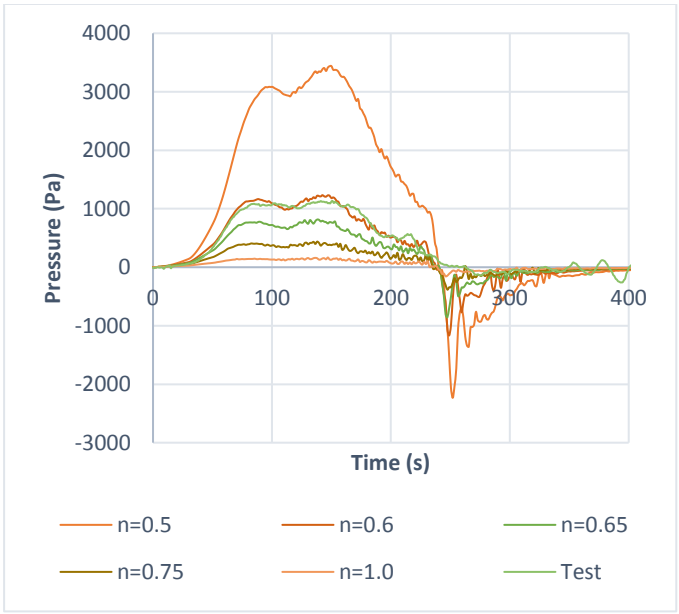

(a) $p_{ref} = 4\ Pa$ and varied exponent

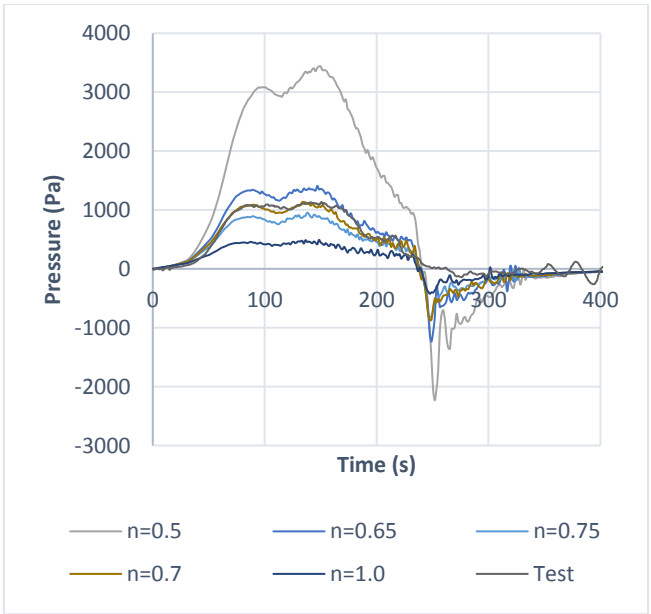

(b) $p_{ref} = 50\ Pa$ and varied exponent

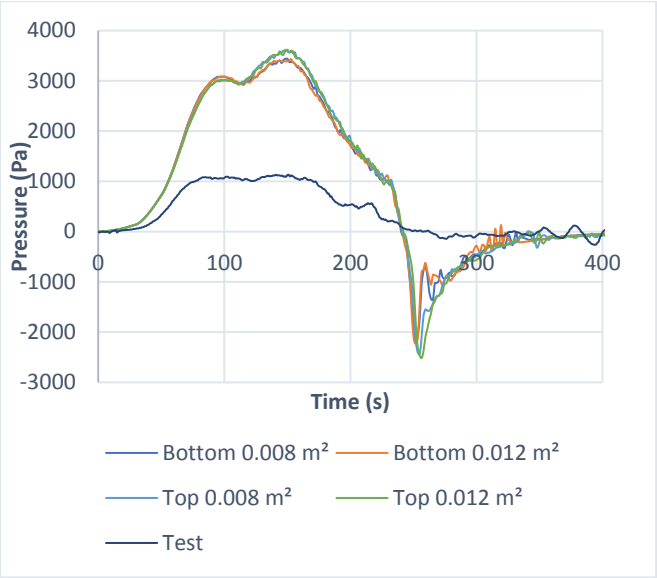

(c) Localized leakage location and area

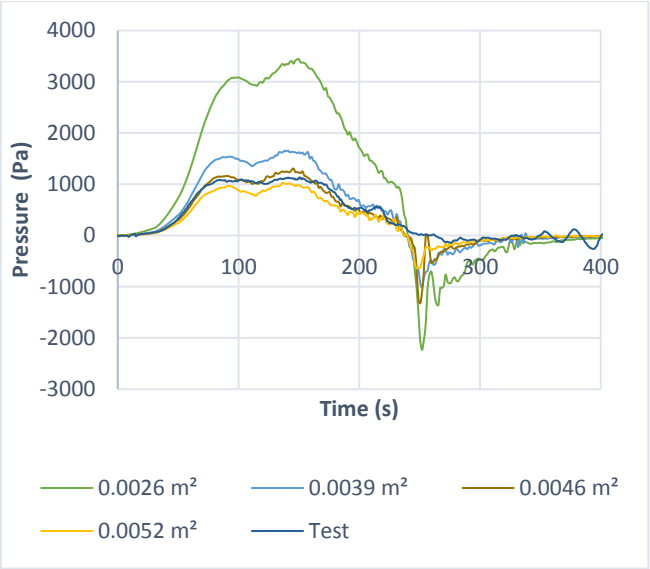

(d) Bulk leakage area

Figure 3.3.4. Comparison of pressure profile in fire room (Test 4)

To analyse the pressure development in the adjacent room, the pressure difference between two rooms is considered and illustrated in Figure 3.3.5. By comparing the results, striking difference between the simulation and test pressure difference profiles can be detected. According to the experimental data, there is pressure difference of about 50 Pa between rooms up to 90 s, followed by rapid decline and identical pressure with the fire room. FDS model also revealed that the peak difference is around 50 Pa, but the growth and decline are smoother. Increasing both localized and bulk leakage areas have a more distinctive effect on the pressure difference profile between two rooms. Whether the localized leak is on top or bottom of the door seems not to influence the parameter under consideration. It can be suggested that experimental pressure difference measurements are not accurate.

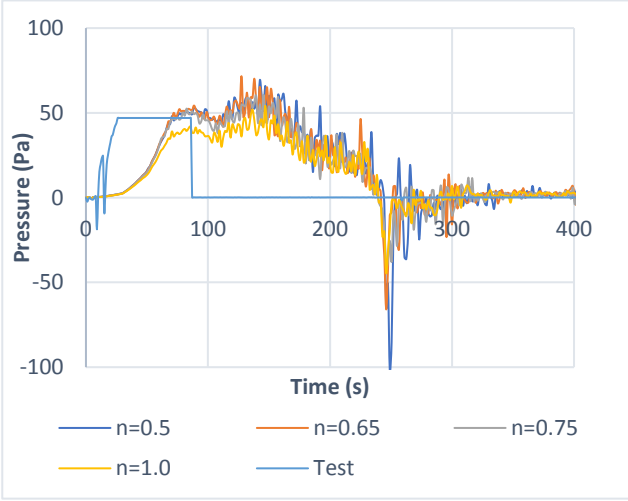

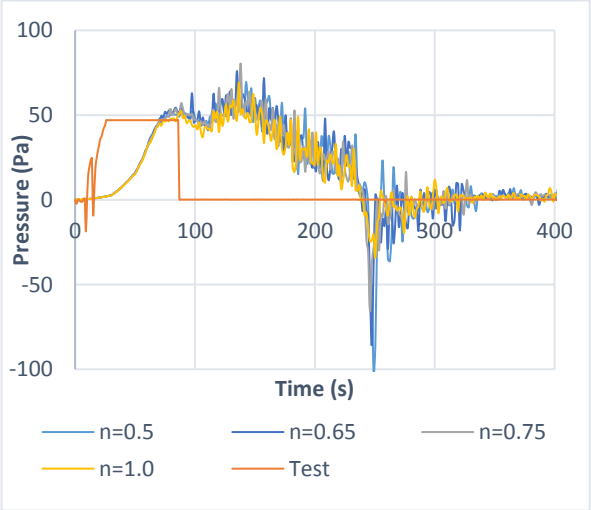

(a) $p_{ref} = 4\ Pa$ and varied exponent

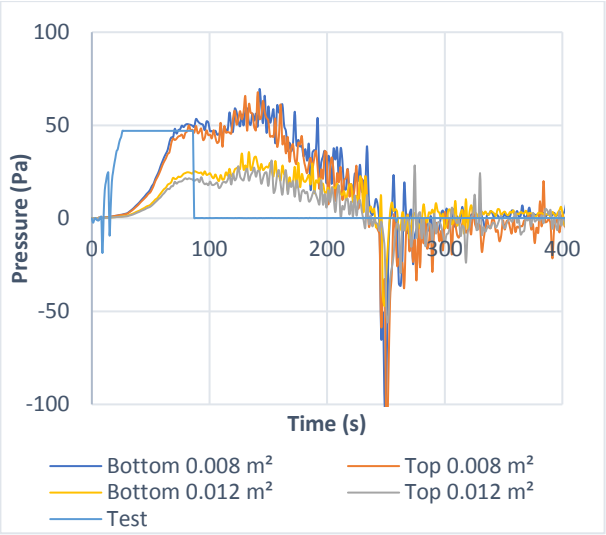

(b) $p_{ref} = 50\ Pa$ and varied exponent

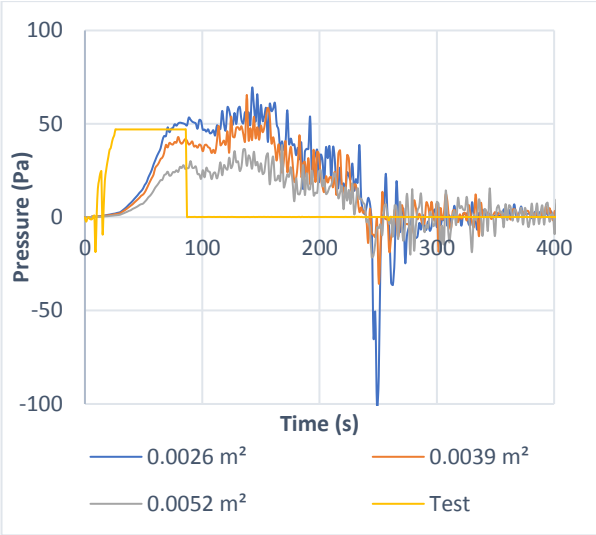

(c) Localized leakage location and area

(d) Bulk leakage area

Figure 3.3.5.Comparison of pressure difference between two rooms (Test 4)

3.3.4 Leakage volume flow rate

The same behaviour as in Test 3 for relationship between enlarging the leak area by changing the exponent value and increasing volume flow rate can be observed for fire room, whereas for adjacent room contrary effect is demonstrated. With reference pressure of 50 Pa, flow out of fire room is insignificantly reduced which is likely to be caused by the lower pressure difference ratio to reference pressure in the equation FDS uses to estimate volumetric flow rate. Flow in can be observed at 240 s which indicates underpressure inside the enclosure.

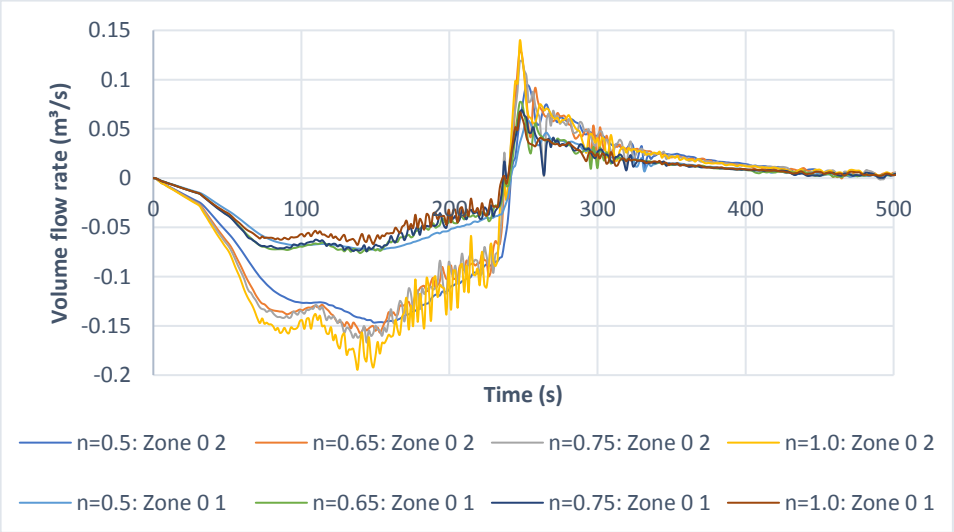

Figure 3.3.6. Comparison of volume flow rate through bulk leakage with $p_{ref} = 4\ Pa$ (Test 4)

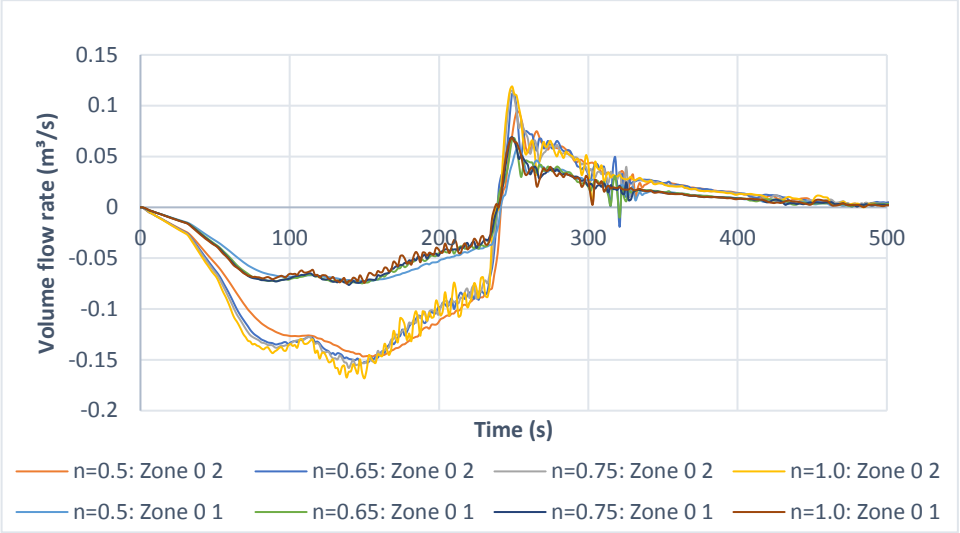

Figure 3.3.7. Comparison of volume flow rate through bulk leakage with $p_{ref} = 50\ Pa$ (Test 3)

Leakage area is the governing parameter as Figure 3.3.8 illustrates: changes to volume flow rate are more prominent with varying the pressure zone leakage area. Since it was found that 0.0046 m^2 is in alignment with experimental data, it can be stated that leakage flow rate out of fire room with the peak of 0.184 m^3/s had possibly occurred during the test.

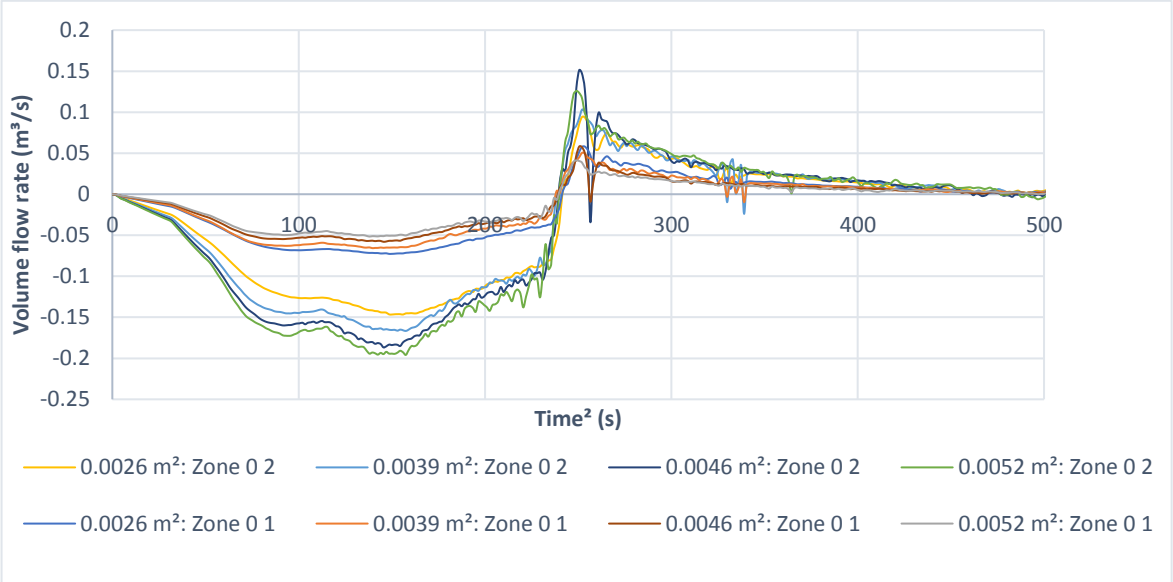

Figure 3.3.8. Comparison of volume flow rate through bulk leakage with varied bulk area (Test 4)

Increase in pressure zone leakage reduces volume flow rate through the aperture on the partition door. It can be due to the lower pressure difference between the two rooms as overpressure will be relieved via larger bulk leakage areas assigned to rooms. Higher flow rate occurs through gap or crack at the top of the door due to smaller density of air.

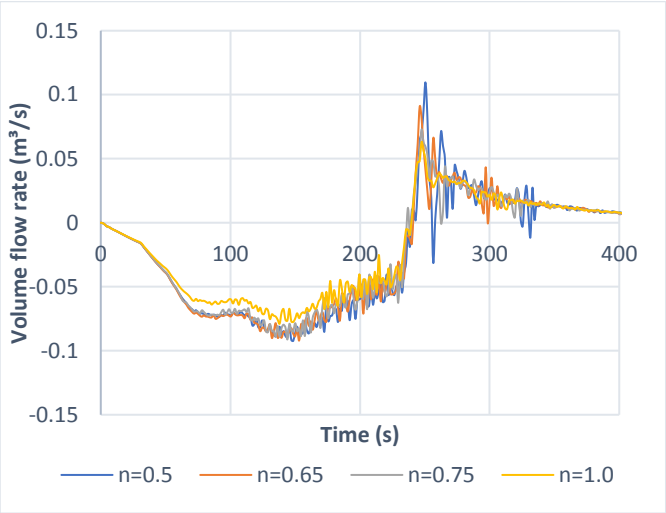

(a) $p_{ref} = 4\ Pa$ and varied exponent

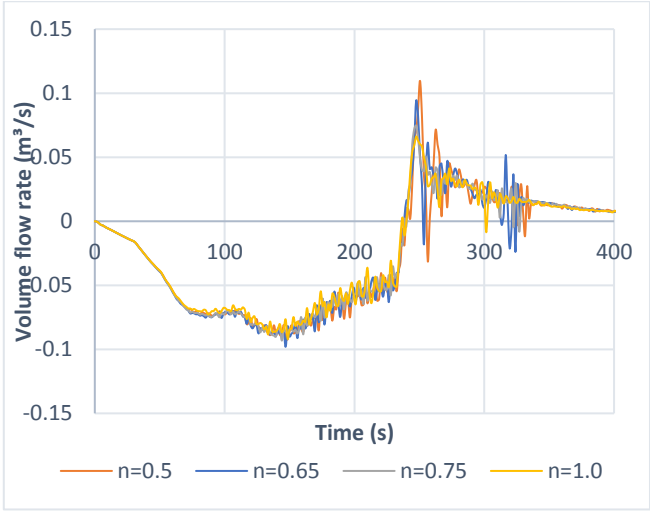

(b) $p_{ref} = 50\ Pa$ and varied exponent

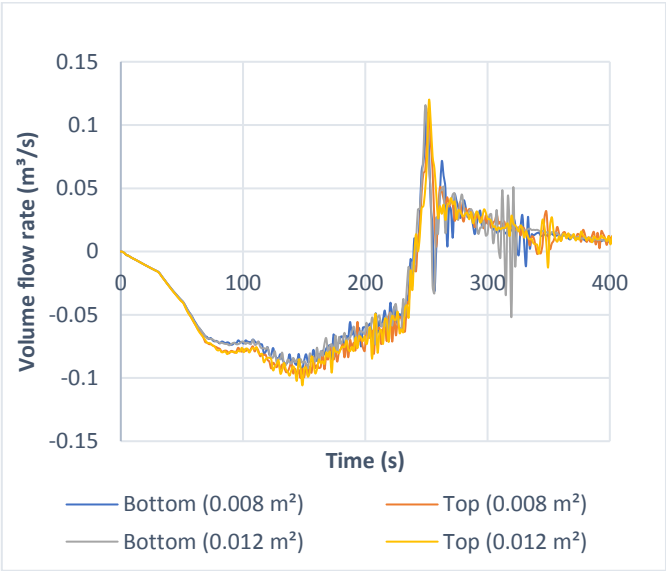

(c) Localized leakage location and area

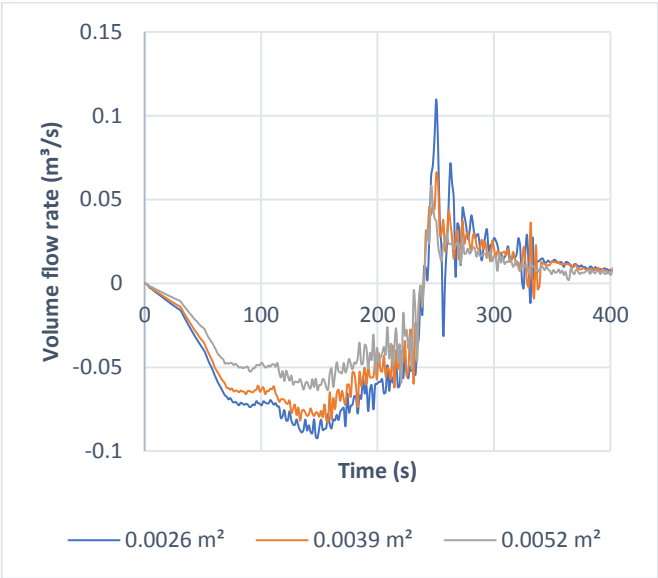

(d) Bulk leakage area

Figure 3.3.9. Comparison of volume flow rate through localized leakage (Test 4)

4. Discussion

4.1 Leakage modelling study

Based on the leakage study performed it can be seen that parameters such as pressure, volumetric leakage flow affected not only by the leakage modelling approach, but also by the location of leakage for both methods and by pressure exponent value for Bulk leakage.

The highest pressure of 20 kPa was obtained with localized leak at the bottom of the door while using bulk leakage with the identical leak location resulted in the lowest pressure of 15 kPa. As can be seen the overpressure values are unrealistically high since the surfaces were assumed to be adiabatic and the leakage area was set to be only 0.001 m^2, while in reality there are more leakage paths around windows and doors and the part of heat produced will be lost to the compartment boundaries. Breakage of windows will also take place with overpressure, thereby creating an opening and relieving pressure, and light-weight structures are likely to fail with 1600 Pa. However, the objective of the study was to analyse the effect of different parameters on the pressure and volumetric leakage flow rate values by keeping the minimum input parameters.

For pressure zone leakage approach, lower pressures and leakage flows were observed for the leak at the bottom of the door compared to the top. This can be explained by the reverse proportionality of volumetric flow and density of flow: the temperature is higher at the top and air density is lower, thereby resulting in higher volume flow through leakage for the leak at the top. This relation can be seen from Eq. (2.7) that is used by FDS for pressure Zone leakage approach. This equation also defines a positive correlation between pressure difference and volumetric flow rate which can also be noticed from the obtained results. Rise and decay of pressure were followed by rise and decay of leakage flow, respectively, which can also be explained by the positive correlation FDS employs for the pressure change and volume flow rate outlined in Eq. (2.7). Changing the default value of `LEAK_PRESSURE_EXPONENT` led to significantly lower pressure rise in the room as it allows leakage area to vary with pressure. Verification of flow rate equation showed that the calculation results of flow rate using ambient density and measured duct volume flow differ considerably, while flow rate calculation results using flow density are more similar with post-processed values.

For localized leakage, even though volume flow rates did not deviate substantially with flow rate for the bottom leak being slightly lower, higher pressures were obtained for the leak at the bottom of the door. The opposite trend was observed compared to the pressure zone leakage: overpressure values were increased when leakage flow rate was lower. It might be claimed that the difference can be caused by the fact that the localized leakage is governed by the total pressure which includes background and perturbation, whereas background pressure controls the pressure zone leakage.

Nevertheless, the values of the total and background pressures obtained by FDS do not deviate considerably. Thus, the reason for this discrepancy was not identified. Similar to the pressure zone leakage, flow rate calculation results employing flow density are in good agreement with post-processed values.

4.2 Validation study

By comparing two tests, it can be seen that overpressure is significantly larger (1000 Pa) when the ducts were closed (Test 4). In addition, using larger fire source also is likely to contribute to higher pressures. Despite the fact that the fans were deactivated, overpressure was reduced to 260 Pa with open ducts (Test 3). Despite that the value exceeds 100 Pa a threshold value for occupants to open the inward opening doors. Therefore, safe evacuation of occupants can be hindered due to overpressure.

By looking at the results of the validation of Mons experiments, the importance of the input parameters can be noticed. To illustrate, using $C_{3.4}H_{6.2}O_{2.5}$ as a chemical formula for the wood, resulted in HRR profile that is not in a good agreement with experimental HRR due to earlier extinction, and HRR is one of the important parameters related to fire development as it governs the environmental effects of fire in an enclosure. Flame extinction in FDS takes place due to decreased temperatures and decrease of the oxygen via suppression algorithm based on the energy released locally: cell temperature should exceed critical flame temperature for combustion to proceed. It has been suggested that the discrepancy can be caused either by the stoichiometry of the reaction with $C_{3.4}H_{6.2}O_{2.5}$: 1 mole of $C_{3.4}H_{6.2}O_{2.5}$ reacts with 3.62 moles of air.

$$C_{3.4}H_{6.2}O_{2.5} + 3.62\ (O_2 + 3.76N_2) \rightarrow 3.31CO_2 + 3.10\ H_2O + 0.01\ CO + 0.07\ C + 13.61\ N_2$$

However, 1 mole of specified CH_2O reacts with 1 mole of air.

$$CH_2O + (O_2 + 3.76N_2) \rightarrow CO_2 + \ H_2O + 3.76\ N_2$$

Therefore, it can be seen that larger volume fraction of air is involved in the burning of $C_{3.4}H_{6.2}O_{2.5}$ which results in more rapid consumption of oxygen and early extinction.

The study proved that Blower Door test results do not correspond to the actual leakage area. Test results are analyzed by using mathematical models to obtain design leakage values. To illustrate, the ASHRAE Handbook of Fundamentals uses 4 Pa as reference pressure which corresponds to the default value in FDS; thus, the values are extrapolated for 4 Pa even though it may lead to inaccurate estimations of volume flow rate because of assumed correlations. In addition, openings and crack areas tend to change with pressure. Despite pressures induced during the test are

significantly higher compared to the normal conditions (50 Pa), the values are not sufficiently high for possible pressure rise induced by fire in passive houses. Therefore, it is expected that the leakage area will increase during a fire in a passive house as was shown by the validation study results.

Pressure results also showed that the overpressure in the enclosure was better captured when the `LEAK_PRESSURE_EXPONENT` parameter was defined as it allows to account for the leakage area change with pressure. However, setting `LEAK_REFERENCE_PRESSURE` to 50 Pa brought about higher pressures in FDS due to reduction of leakage area. As a consequence, higher values of the flow exponent were required to match the experimental data.

The validation study also demonstrated the importance of leak area for pressure zone leakage method. With arbitrarily increased leakage areas, the results were in good agreement with 0.0046 m^2 for Test 4. However, it can be suggested to employ `LEAK_PRESSURE_EXPONENT` and `LEAK_REFERENCE_PRESSURE` to take into account the increase in leakage area with overpressure unless the leakage area is measured at overpressures comparable to fire with more powerful fans.

Location and area of localized leak as well as bulk leak area were found to be influential parameters for pressure difference between two rooms. It is likely that the leak area around the door is larger than assumed 0.008 m^2 as higher pressure difference values were obtained in FDS. It should be noted that pressure in adjacent room is comparable to the pressure in fire room. Occupants in adjacent room are also likely to experience evacuation problems: overpressure exceeds 100 Pa at 180 s and 40 s during Test 3 and 4, respectively. 0.004 m^2 was found to be critical localized leak area below which pressure difference between two rooms was significantly larger in thesis by Orozco Cruz.

Increase in bulk leakage area with both flow exponent and constant area value resulted in higher leakage flows out of the fire room, while flow rate out of the adjacent room was reduced. Volume flow rate through a leakage is governed by the leak area, pressure difference between the room and ambient, and air density. It might be suggested that lower leakage area in adjacent room compared to fire room is the reason for this phenomenon. However, the bulk leakage area in adjacent room was set to 0.0013 m^2 for the total bulk leakage areas of 0.0039 m^2 and 0.0052 m^2,and still flow rate is diminished. Therefore, it might be caused by lower overpressure values in adjacent room. For $p_{ref} = 50\ Pa$, changing the default exponent value had less effect on the volume flow rate through bulk leakage. It can be due to the reduced pressure ratio in Eq. (2.8) and subsequent

decrease in leakage area which is directly proportional to the volume flow rate through leakage as shown in Eq. (2.7).

For localized leakage, volumetric flow rate was reduced with the increase in the constant area of bulk leakage. This can be explained by lower pressure difference between two rooms which is the main driving force for the flow to occur. Similar to the leakage study, difference in the density of flow through leakage due to location of the leak is responsible for the lower flow with leak at the bottom of the door. Unexpectedly, changing area of the leak did not lead to the difference in the localized leakage flow.

4.3 Uncertainties and Limitations

It is important to take into account both experimental and modelling uncertainties. Experimental uncertainties are associated with measurements. To illustrate, HRR esymated by mass loss rate measuremnts can differ from the actual HRR. In addition, lack of experimental data also introduces uncertainties to the model. In this study, detailed information about the ventilation system was not available apart from length and diameter of the ducts. In addition, there is an uncertainty in thermal properties of the materials adopted in the model.

Modelling uncertainties are associated with HVAC pressure solution being not directly coupled to FDS Hydrodynamics solver: implicit coupling based on wall boundary conditions is employed for HVAC vents [19]. Another limitation of FDS is associated with pressure solver: a no-flux boundary condition, zero velocity normal to the boundary, is imposed at the solid surfaces that are not part of the boundary of the computational domain [19]. This caused low volumetric flow rate in the ducts in the Test 3 validation study as was shown in the previous section. Moreover, basic extinction model employed in FDS resulted in early extinction of fire in Test 4 due to oxygen reduction. Unfortunately, CFD results for oxygen consumption cannot be compared to the experimental as gas analyzers failed to measure the concentration of gases during the tests.

Limitation of this study include not performing an extensive analysis of fuel and fire related parameters, not assessing the uncertainties associated with thermal properties of the materials, and not checking the sensitivity of model to HVAC loss coefficients. Mass storage and energy transport in the ducts were also not taken into account in the model as FDS 6.5.2 was used to perform validation study. In current FDS 6.6.0 version setting `HVAC_MASS_TRANSPORT=TRUE` allows to account for mass storage and energy transport in ducts [19]. In addition, the production of CO was not analysed in this work as no experimental data was available to compare the generation of combustion gases. According to the master thesis of Kallada Janardhan, default simple chemistry model cannot capture well the production of CO is in ventilation controlled fires [13].

5. Conclusions

In conclusion, study showed that the localized leakage results in higher pressures compared to pressure zone leakage. In addition, the location of the leak was found to affect both overpressure and volumetric leakage flows. The importance of the flow exponent value was also identified.

For the validation study, two tests with different ventilation configuration were under analysis: with no ventilation (closed pipes) and with deactivated fans (open pipes). The study showed that overpressure cannot be well predicted by the constant leak area based on the Blower door. However, introducing parameters such as flow exponent and reference pressure allows to obtain a good agreement with experimental data. Therefore, these two parameters should be accurately defined during Blower door test and inputted in FDS instead of default values.

Both leakage modelling approaches were used in the model. Regarding the bulk leakage method, the study showed the sensitivity of pressure and flows out of the compartment to parameters such as area, the flow exponent, and reference pressure. Larger reference pressures resulted in higher overpressures and larger exponent values required to match the experimental results. The influence of the bulk leakage area value on the volumetric flow rate through localized leak was discovered to be larger than the position and area of the leak. Despite being separated by a partition door, overpressure in both rooms were comparable. Location and area of localized leak as well as the area of the bulk leak are the major parameters that affected the pressure difference values obtained by FDS.

More research can be done to take into account the uncertainties associated with input parameters related to fire characteristics and ventilation configuration. The effect of more complex ventilation system with multiple components can be studied as well. Advanced extinction and chemistry models can also be adopted for better prediction of underpressure and concentration of combustion gases.

References

[1] European Union, Energy Performance of Buildings, Counc. Dir. (2010) 13–35. http://eur-lex.europa.eu/legal-content/EN/TXT/?uri=LEGISSUM:en0021 (accessed January 18, 2018).

[2] European Union Law, Energy efficiency: energy performance of buildings, EUR-Lex. (2002) 1. http://eur-lex.europa.eu/legal-content/EN/TXT/?uri=LEGISSUM%3Al27042 (accessed January 18, 2018).

[3] P. Institute, What is a passive house?, (n.d.). http://www.passiv.de/old/07_eng/PHI/Flyer_quality_assurance.pdf (accessed January 19, 2018).

[4] B.D. Van Dam, M. Van Huet, Passive Housing, 2015. https://sustainabledevelopment.un.org/content/documents/5744Passive Housing.pdf.

[5] PassREg, Defining the Nearly Zero Energy Building: Passive House + renewables, 2015. https://ec.europa.eu/easme/sites/easme-site/files/Defining the Nearly Zero Energy Building.pdf.

[6] S. Attia, E. Mlecnik, S. Van Loon, Principles for Nearly Zero Energy Building in Belgium, 2011. https://orbi.ulg.ac.be/bitstream/2268/167472/1/Attia_WSED2012_Belgium.pdf.

[7] D. Vanhaverbeke, P. Prof, S. Welch, Fire development in passive houses : qualitative description and design of full-scale fire tests, 2015.

[8] T.A. Reddy, J.F. Kreider, P. Curtiss, A. Rabl, Heating and cooling of buildings : principles and practice of energy efficient design, n.d. https://books.google.be/books?id=uwwNDgAAQBAJ&dq=4+Pa+reference+pressure+leak+door+test&hl=ru (accessed April 30, 2018).

[9] ASTM International, Standard Test Methods for Determining Airtightness of Buildings Using an Orifice Blower Door, 2015. doi:10.1520/E1827-11.2.

[10] L. Audouin, L. Rigollet, H. Prétrel, W. Le Saux, M. Röwekamp, OECD PRISME project: Fires in confined and ventilated nuclear-type multi-compartments - Overview and main experimental results, Fire Saf. J. 62 (2013) 80–101. doi:10.1016/j.firesaf.2013.07.008.

[11] H. Prétrel, W. Le Saux, L. Audouin, Pressure variations induced by a pool fire in a well-

confined and force-ventilated compartment, Fire Saf. J. 52 (2012) 11–24. doi:10.1016/j.firesaf.2012.04.005.

[12] J. Wahlqvist, P. Van Hees, Validation of FDS for large-scale well-confined mechanically ventilated fire scenarios with emphasis on predicting ventilation system behavior, Fire Saf. J. 62 (2013) 102–114. doi:10.1016/j.firesaf.2013.07.007.

[13] R.K. Janardhan, Fire Induced Flow in Building Ventilation Systems, 2016.

[14] S. Hostikka, R.K. Janardhan, U. Riaz, T. Sikanen, Fire-induced pressure and smoke spreading in mechanically ventilated buildings with air-tight envelopes, Fire Saf. J. 91 (2017) 380–388. doi:10.1016/j.firesaf.2017.04.006.

[15] S. Hostikka, R.K. Janardhan, U. Riaz, T. Sikanen, FIRE MODELLING OF ENERGY-EFFICIENT Consideration of air-tightness and mechanical, n.d.

[16] Y.Z. Li, CFD modelling of pressure rise in a room fire, 2015.

[17] C. Fourneau, N. Cornil, C. Delvosalle, H. Breulet, S. Desmet, S. Brohez, Comparison of fire hazards in passive and conventional houses, Chem. Eng. Trans. 26 (2012) 375–380. doi:10.3303/CET1226063.

[18] P. Berthelot, Etude expérimentale du développement d ' un incendie dans une maison basse énergie, 2016.

[19] K. Mcgrattan, R. Mcdermott, Sixth Edition Fire Dynamics Simulator User ' s Guide, 2016. doi:10.6028/NIST.SP.1019.

[20] E. Gissi, An Introduction to Fire Simulation with FDS and Smokeview, Creat. Commons Attrib. Alike 3.0. (2009) 164. http://creativecommons.org/licenses/by-sa/3.0/.

[21] K. McGrattan, S. Hostikka, R. McDermott, J. Floyd, C. Weinschenk, K. Overholt, Fire Dynamics Simulator, Technical Reference Guide, Volume 1: Mathematical Model, NIST Spec. Publ. 1018. 1 (2013) 175. doi:10.6028/NIST.SP.1018-1.

A. APPENDIX: Leakage modelling study

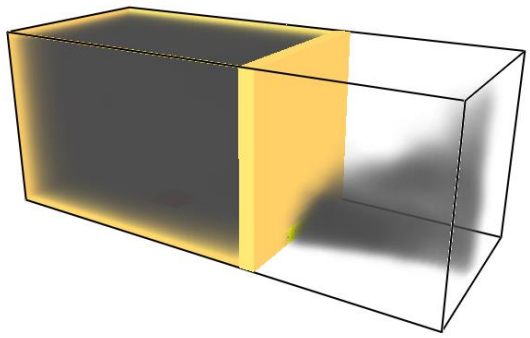

(a) Bulk leakage at the bottom

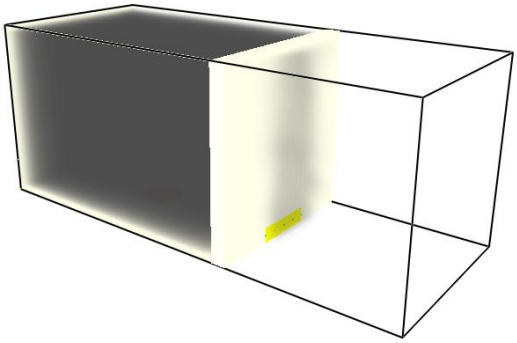

(b) Localized leakage at the bottom

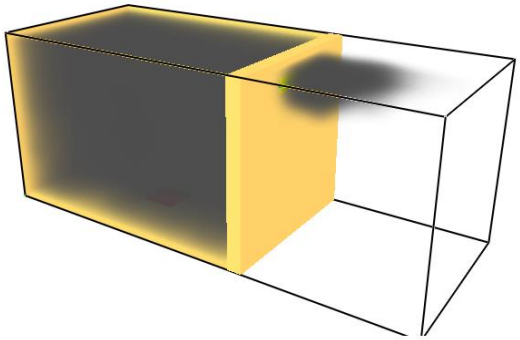

(c) Bulk leakage at the top

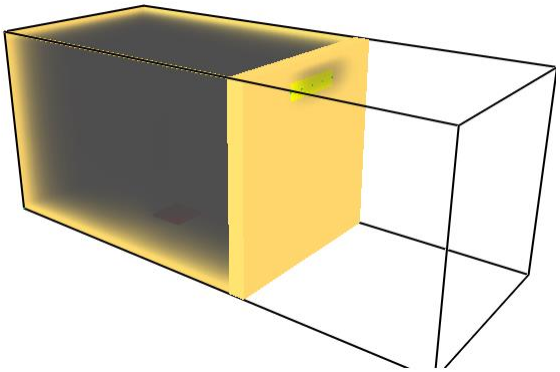

(d) Localized leakage at the top

Figure 4.3.1 Visualization of leakages in Smokeview

B. APPENDIX: TEMPERATURE

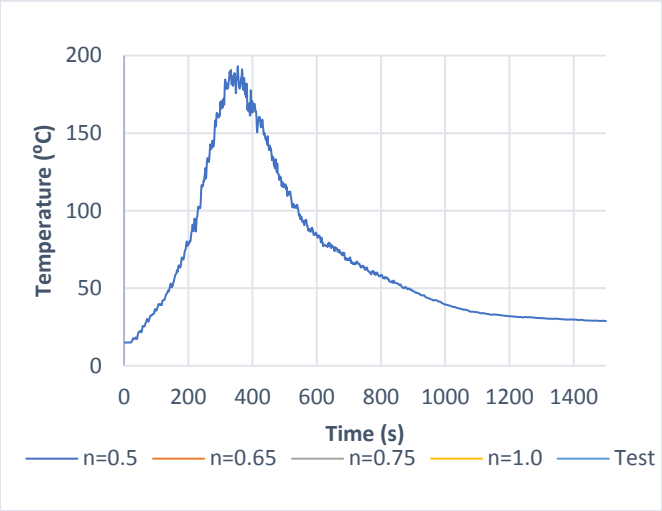

(a) $p_{ref} = 4\ Pa$ and varied exponent

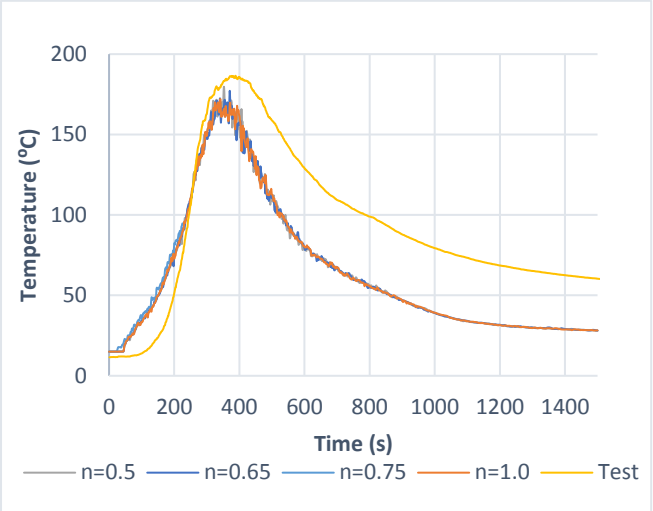

(b) $p_{ref} = 50\ Pa$ and varied exponent

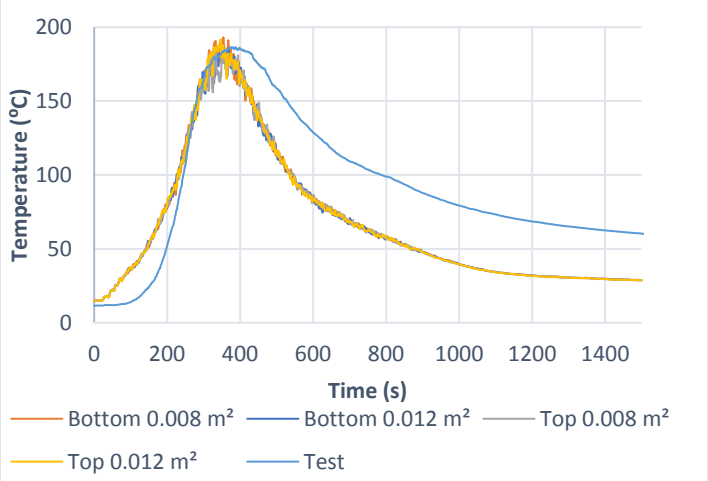

(c) Localized leakage location and area

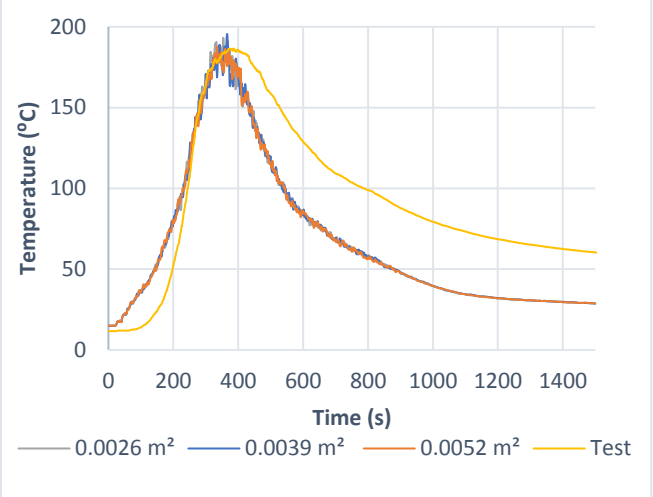

(d) Bulk leakage area

Figure 4.3.1. Comparison of room temperature in fire room at 1.8 m (Test 3)

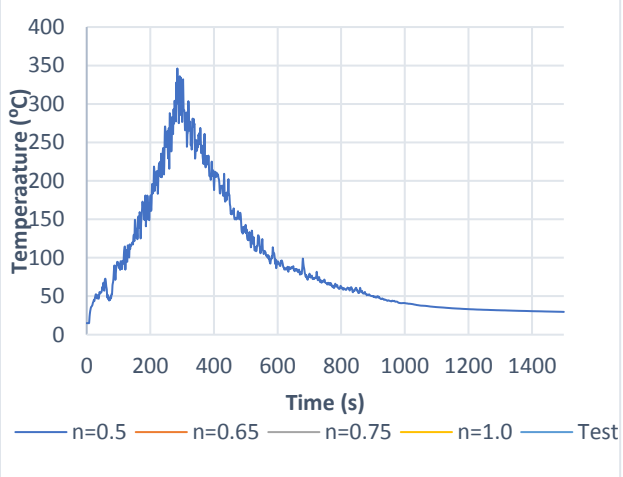

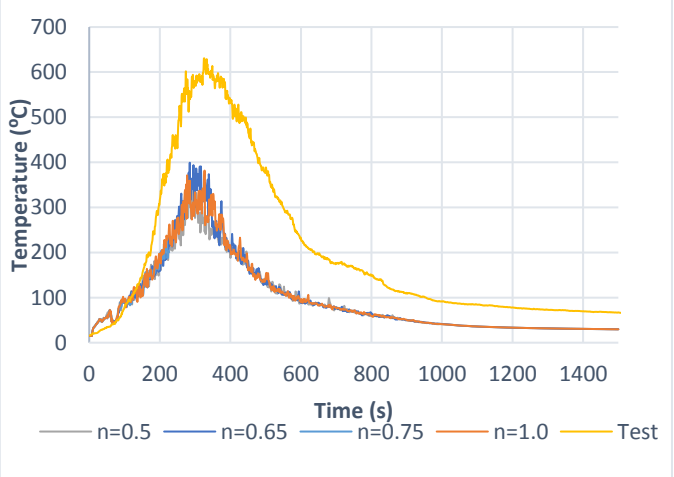

(b) $p_{ref} = 4\ Pa$ and varied exponent

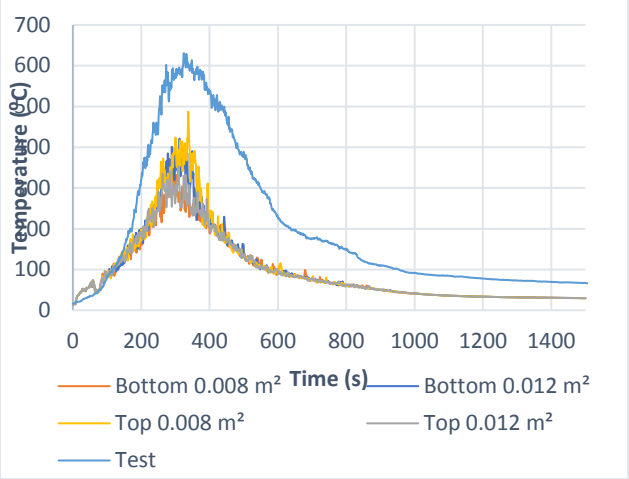

(c) $p_{ref} = 50\ Pa$ and varied exponent

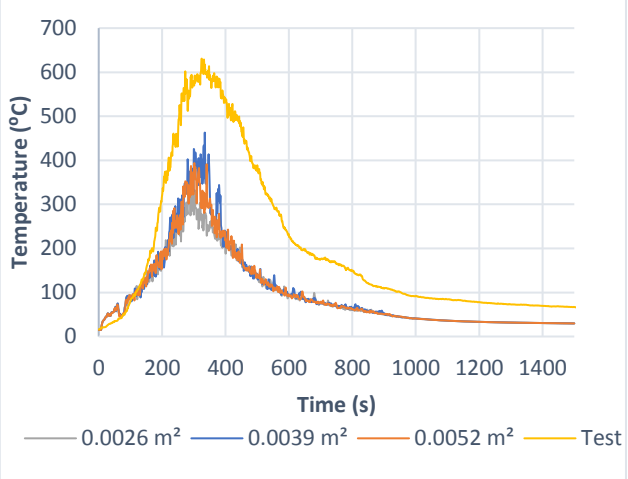

(d) Localized leakage location and area

(e) Bulk leakage area

Figure 4.3.2. Comparison of temperature above fire (Test 3)

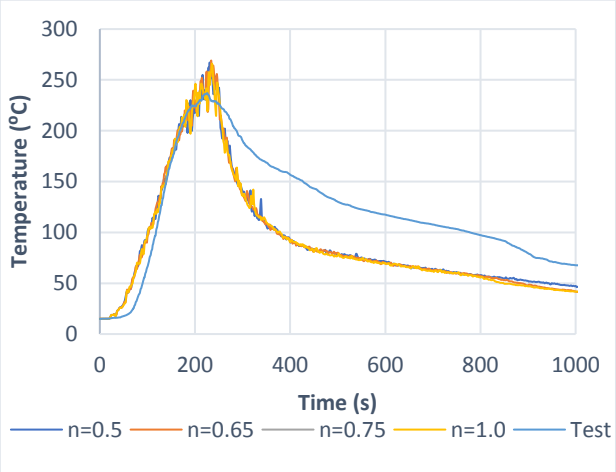

(a) $p_{ref} = 4\ Pa$ and varied exponent

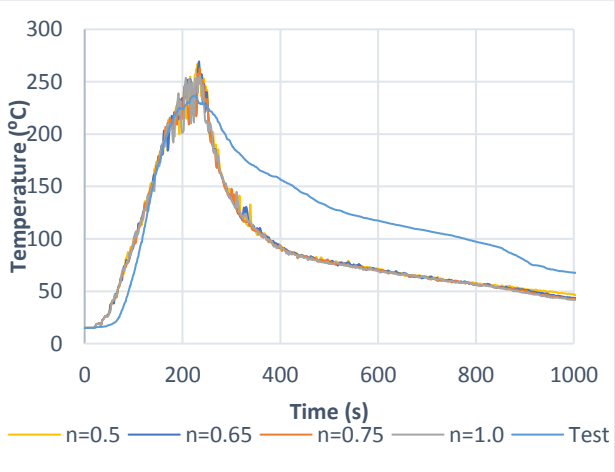

(b) $p_{ref} = 50\ Pa$ and varied exponent

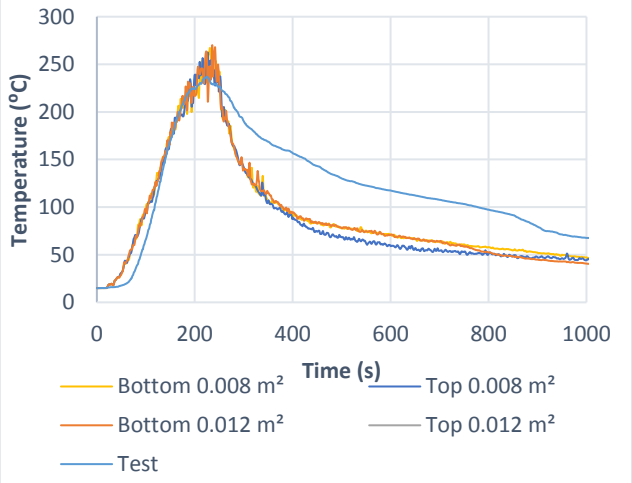

(c) Localized leakage location and area

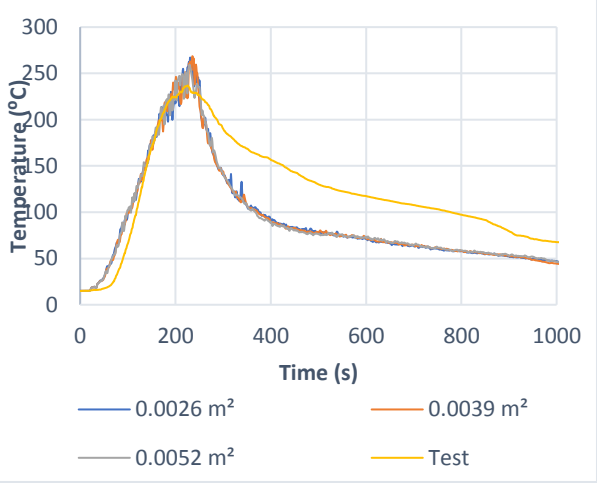

(d) Bulk leakage area

Figure 4.3.3. Comparison of room temperature in fire room at 1.8 m (Test 4)

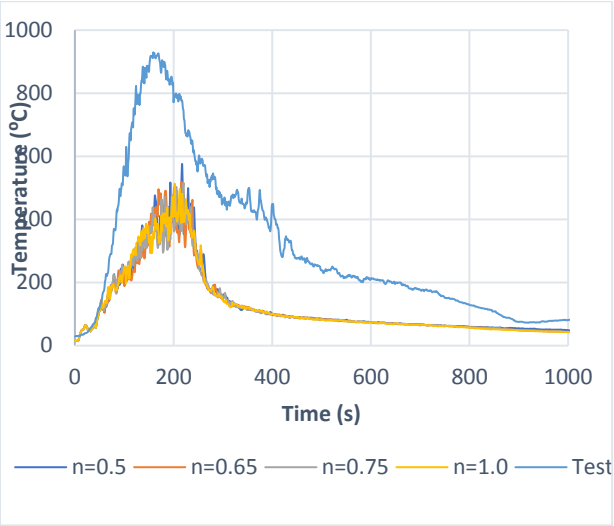

(a) $p_{ref} = 4\ Pa$ and varied exponent

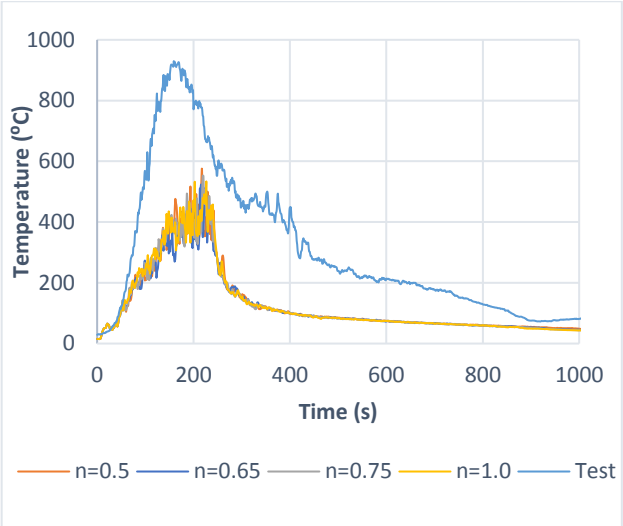

(b) $p_{ref} = 50\ Pa$ and varied exponent

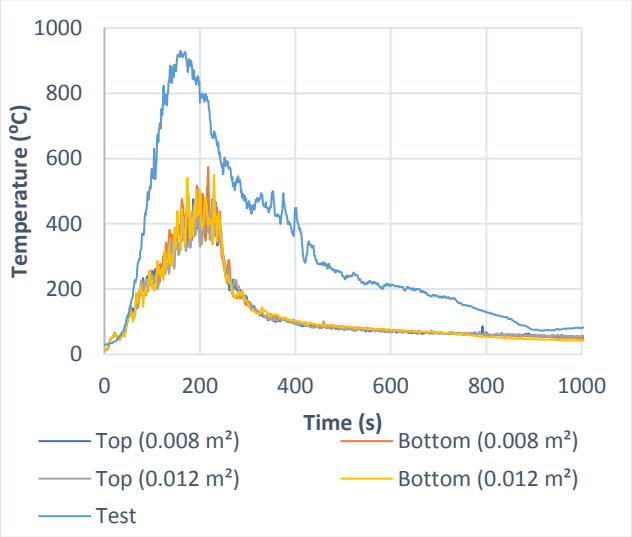

(c) Localized leakage location and area

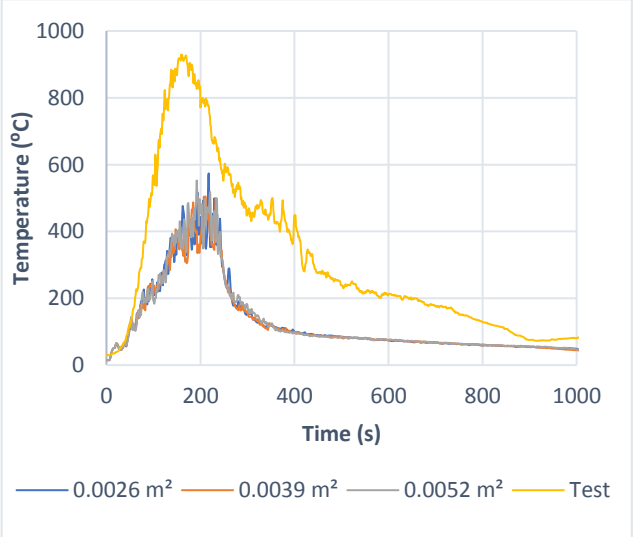

(d) Bulk leakage area

Figure 4.3.4. Comparison of temperature above fire (Test 4)